CONTRIBUTIONS OF THE DELTOID AND ROTATOR CUFF TO SHOULDER MOBILITY AND STABILITY: A 3D FINITE ELEMENT ANALYSIS

A DISSERTATION
SUBMITTED TO THE DEPARTMENT OF MECHANICAL ENGINEERING
AND THE COMMITTEE ON GRADUATE STUDIES
OF STANFORD UNIVERSITY
IN PARTIAL FULLFILLMENT OF THE REQUIREMENTS
FOR THE DEGREE OF
DOCTOR OF PHILOSOPHY

Joshua Dale Webb

August 2011

This dissertation is online at: http://purl.stanford.edu/cy150tn9705

I certify that I have read this dissertation and that, in my opinion, it is fully adequate in scope and quality as a dissertation for the degree of Doctor of Philosophy.

Scott Delp, Primary Adviser

I certify that I have read this dissertation and that, in my opinion, it is fully adequate in scope and quality as a dissertation for the degree of Doctor of Philosophy.

Ellen Kuhl

I certify that I have read this dissertation and that, in my opinion, it is fully adequate in scope and quality as a dissertation for the degree of Doctor of Philosophy.

Silvia Blemker

Approved for the Stanford University Committee on Graduate Studies.

Patricia J. Gumport, Vice Provost Graduate Education

This signature page was generated electronically upon submission of this dissertation in electronic format. An original signed hard copy of the signature page is on file in University Archives.

Abstract

The shoulder is one of the most mobile and complex joints in the body. The shoulder bones provide few constraints on motion; therefore, stability must be maintained by muscles and ligaments. The mobility of the shoulder allows great versatility, but also makes it prone to injury. A better understanding of the role of the muscles in shoulder mechanics is needed to improve the treatment of shoulder injuries and pathologies. Computational models provide a valuable framework for investigating complicated mechanical systems and characterizing joint mechanics. Previous shoulder models have used simple representations of muscle architecture and geometry that may not capture the details of muscle mechanics needed to fully understand muscle function. The purpose of this dissertation was to create a detailed 3D finite element model of the deltoid and the four rotator cuff muscles. This model was then used to characterize the muscle contributions to joint motion and stability.

The model was constructed from magnetic resonance images of a healthy shoulder. From the images, the 3D geometry of the muscles, tendons and bones was acquired. A finite element mesh was constructed using hexahedral elements. The 3D trajectories of the muscle fibers were approximated and mapped onto the finite element mesh. A hyperelastic, transversely-isotropic material model was used to represent the nonlinear stress-strain relationship of muscle. Bone motions were prescribed and the resulting muscle deformations were simulated using Nike3D, an implicit finite element solver.

To characterize muscle contributions to joint motion, we calculated moment arms for each modeled muscle fiber. The moment arm indicates the mechanical advantage of

activating a fiber and its potential contribution to the resulting joint moment. We found that 3D finite element models predicted substantial variability in moment arms across fibers within each muscle, which is not generally represented in line segment models. We also discovered that for muscles with large attachment regions, such as deltoid, the line segment models under constrained the muscle paths in some cases. As a result, line segment based moment arms changed more with joint rotation than moment arms predicted by the 3D models.

Glenohumeral instability is a common clinical problem which is difficult to treat. To better understand the mechanics of instability we used the model to investigate the role of the muscles in stabilizing the glenohumeral joint. This was done by simulating an imposed 1 cm translational displacement of the humeral head in the anterior-posterior and superior-inferior directions relative to the glenoid. We found that at the neutral position, the anterior deltoid provides the largest potential to resist anterior translation. This counters the conclusions of conventional line segment based models, and is the result of compression generated by muscle contact, which must be considered when characterizing the ability of muscle to resist joint translation.

This dissertation provides a new computational method for analyzing shoulder mechanics, and demonstrates the importance of 3D analysis when investigating the complex function of shoulder muscles.

Acknowledgements

As I look back on my time here at Stanford, there is so much I am grateful for. It has been a wonderful chapter in my life and I am truly privileged to have studied and worked here. First and foremost, I want to say thank you to Scott Delp for being willing to serve as my mentor and advisor. Scott has taught me so much as a scientist, a mentor, a father, and a friend. Not only has he been a wonderful mentor in the areas of shoulders, musculoskeletal modeling, and research, but also a great mentor about life in general. Thanks so much Scott for the time you have invested in me. It has been an honor and a pleasure to work with you.

Silvia Blemker has been an inspiration to me as I have watched her progress from grad student to post-doc to professor. As the developer of the constitutive model for muscle, and guru of both finite elements and imaging, she has been my greatest source of technical help. I am so grateful to her for willingly sharing her code with me, patiently responding to frantic or frustrated emails, serving on my reading committee, and for being such a good friend and mentor.

Thanks also to Garry Gold for being the first person to hire me as a master's student. Though this project did not end up using as much imaging as I hoped, Garry has always been willing to help me with the imaging related parts of my project. I am grateful to him for his support, and for being willing to serve on my defense committee.

I am also grateful to Ellen Kuhl for taking time to be on my reading committee, and my defense committee. I learned a lot about finite elements by sitting in on her class, and her Simbios talks were amazing.

I have been surrounded by so many good friends in the Neuromuscular Biomechanics Lab (NMBL). I have many fond memories from my interactions with you all. You all have been some of my closest friends, my biggest cheerleaders, and a great wealth of technical information on virtually any topic. I hope our friendships and collaborations continue on into the future. Thanks in particular to all of you willing to go rock climbing with me.

Of the many excellent teachers I have had through the years, there were two undergraduate professors that really inspired me to be the best I could be and to work harder than I thought possible. Takashi Nakajima first challenged me with his physics courses at Palomar College. He demanded so much…a thorough knowledge of calculus, personal preparation for labs, real teamwork, and self-discipline for homework. Without those skills, I doubt I would be here now. Roger Gonzalez upped the ante with his Dynamics course at LeTourneau University. That was the first class that I wondered if I could really pass (but certainly not the last time I would think such a thought). He inspired me to work hard, and to be inquisitive. He mentored my senior design research project studying ACL strain and introduced me to biomechanics and dynamic simulation. The ability to simulate human motion and learn from it is an area that fascinated me then, and still fascinates me now. I am thankful to have had the opportunity to work on biomechanics simulations here.

I am also grateful to my parents for their support and hard work to help me get to this place in life. My mother left a lucrative career as a physical therapist to home school my brothers and me at a time when that was highly unusual. My parents have always encouraged us to think outside the box, and to pursue our interests wholeheartedly. I

appreciate the sacrifices they have made to ensure our success. My dad is the model of a man who works hard and does his best in every circumstance. They recently celebrated their 40th anniversary, and I have been privileged to have such amazing and dedicated parents, and supportive brothers. I truly could not ask for a better family.

I am grateful for the friends we have made in the bay area as well. Ashley & Andy Gillard, and Brian & Betty Mooney will be lifelong friends. Andy and Brian were a constant source of fun, whether we were mountain biking, grilling, playing board games, or just hanging out. They were there for me when I needed a listening ear, a glass of wine, technical advice, or to be relentlessly dragged up some mountain trail outside of Santa Cruz. I think we still owe both the Mooneys and the Gillards about 3 yrs of free babysitting as well. Watching our kids so we could go out on dates was such a generous gift on their part. They will never know what a tremendous help that was, but it certainly enabled me to be a better husband, father, and student. I am also grateful for the opportunity to play music at Peninsula Bible Church. It was always refreshing to me to play the bass and hang out with good friends. I also greatly appreciate the Dodson's and the Sid's for letting me live with them the last two summers while I have been writing this dissertation. As the old saying goes, "Fish and houseguests smell after three days." They have patiently put up with me for weeks at a time, and I am grateful for their generous hospitality.

None of this would have been remotely possible without the loving support of my beautiful wife Bethany. I have the good fortune of having a technically minded wife who understands when I talk on and on about moment arms, convergence, inverting elements, or kinematics. She has patiently put up with the long hours of work, and she always

knows when I need to take a break, when I need to buckle down and work harder, or when I just need to go mountain biking with friends. She has been a faithful friend, a wonderful wife, and the best mother I have ever seen. There is no way to put into words how much she means to me. She is truly the joy and love of my life. I love you!

During the course of graduate school, I have been blessed with the birth of four wonderful children: Nathan, Isaac, Hannah, and Ella. They bring me such joy, and I am so proud of each one of them. I love each of you! Watching them grow and develop has been an endless source of biomechanical hypotheses, and a refreshing chance to see the world from a new set of eyes. I must confess that I was a bit concerned having them grow up in the 6th Man section of basketball games (with the intriguing new phrases they learned there), and aspiring to grow up and be in the Stanford band (though I'm not sure growing up is required). On a serious note, Stanford has provided a wonderful place to raise our kids, and I hope they remember and treasure at least a few memories of our time here, because I certainly do.

A special thank you is also due to Jeff Weiss, Steve Maas, and Ben Ellis for their assistance in refining the muscle material model and finite element support. This work has been supported by National Institute of Health Grant # R01EB006735 and a National Science Foundation Graduate Fellowship. Computing resources were provided by National Science Foundation award CNS-0619926. Musculoskeletal images in Figure 1.1 are used by permission from the University of Washington "Musculoskeletal Atlas: A Musculoskeletal Atlas of the Human Body" by Carol Teitz, M.D. and Dan Graney, Ph.D.

Joshua Webb
Stanford, California
August 2011

Table of Contents

TABLES

ILLUSTRATIONS

Chapter 1

Introduction

The shoulder is one of the most mobile and versatile joints in the body. While often thought of as a single joint, it is comprised of three bones and four joints in a closed kinematic chain. It has a large range of motion because the articulating bony geometry provides little constraint on joint motion. The glenohumeral joint is often described as a golf ball on a tee, with the humeral head having about 3 times the surface area of the glenoid on which it articulates[7]. Instead of hard restraints, the joint is dynamically controlled through a system of muscles and ligaments. There are 20 muscles crossing the shoulder, and these muscles must coordinate their activations and force production in such a way as to generate joint motion while maintaining a stable base of support for the arm. This dynamically controlled joint design provides an outstanding balance of flexibility and stability while allowing large forces to be generated by the arm through a large range of motion. Working together, this complex system allows for our upper limbs to perform highly-precise fine-motor skills such as playing a musical instrument. The shoulder also supports highly-dynamic motions such as pitching a ball, martial arts throws, or lifting ones body weight (as in rock climbing).

Unfortunately, the precise balance of forces in the shoulder is often disrupted through injury or disease. Shoulder injuries are common and may include dislocation, chronic instability, rotator cuff tears, and impingement. In addition to the active support of the musculature, shoulders are also stabilized by passive mechanisms including the ligaments, joint capsule, the glenoid labrum, cartilage, and negative inter-articular pressure.

Due to the complexity of the joint, and the many tissues involved in joint function, shoulder injuries are notoriously difficult to diagnose and treat. Medical imaging does not always reveal an obvious diagnosis, and many clinical exams lack specificity. Therefore, diagnosis is difficult and must be systematically deduced from a variety of symptoms and tests. Surgical and non-surgical treatments have highly variable outcomes, with many injuries reoccurring. For example, in the case of a shoulder dislocation in a person under 20 years of age, the likelihood of a subsequent dislocation has been reported to be between 45-95% [99]. Chronic shoulder instability, particularly anterior instability, commonly develops after a dislocation. In order to restore joint stability, surgical procedures may be performed. One of the most common stabilization surgeries is the Bankart repair, which reattaches the anterior labrum and capsule to the glenoid[78]. The joint capsule and ligaments are often simultaneously tightened if it is thought that they have been stretched. A Bankart repair results in a range of motion loss[26,78] and may fail to stabilize the joint. Hayashida et al.[40] found that Bankart repair failed to restore stability, or injury reoccurred in 18% of procedures performed arthroscopically, while Mishra and Fanton[76] reported a 7% failure rate, and Grana et al.[35] reported a 44% failure rate for the same procedure.

Muscles play an important role in actuating and stabilizing the shoulder. In the mid ranges of motion the ligaments and capsule are slack, and muscles provide the primary support for joint stability[64]. At the end ranges of motion, when the ligaments and capsule engage, the rotator cuff muscles still provide significant support[64]. As muscles generate force to produce motion, they must simultaneously be coordinated to provide appropriate forces for maintaining stability. This mechanism may fail during a bilateral

anterior shoulder dislocation, which can occur when attempting a bench press exercise with excessive weight[54]. Normal scapular kinematics can be disrupted by the bench, and the pectoralis major can generate enough force to dislocate the humeral head anteriorly. The forces that shoulder muscles must balance can be quite large, due to dynamic joint forces, and the long moment arm between the hand and the shoulder. Bergmann et al. used instrumented shoulder replacements to measure joint reaction forces, and measured shoulder contact loads in excess of body weight resulting from something as simple as picking up a coffee pot[8,106,107]. Given the complexities of the human shoulder, we need to understand the underlying mechanics of the muscular system, and the function which they provide, in order to accurately diagnose and effectively treat shoulder pathologies.

In this dissertation, we chose to focus on the rotator cuff and deltoid (Figure 1.1). The rotator cuff is comprised of four muscles inserting on the humeral head (Figure 1.2). Its main functions are to provide compressive force which keeps the humeral head centered on the glenoid, and generating internal-external shoulder rotation, a motion associated with many shoulder pathologies. Deltoid was included because it is one of the largest shoulder muscles, and is important in shoulder abduction, internal-external rotation, and stabilization[3,36,37,62,109].

There are many methods available to investigate muscle and joint mechanics. Electromyography (EMG) is a useful tool for investigating the timing and activations of muscle, and has been used to quantify the relative contributions of muscles to joint moments[9,21]. EMG allows direct measurement of electrical muscle activity, and gives insight into muscle coordination and neuromuscular control. However, EMG is not very useful when it comes to investigating forces within tissue.

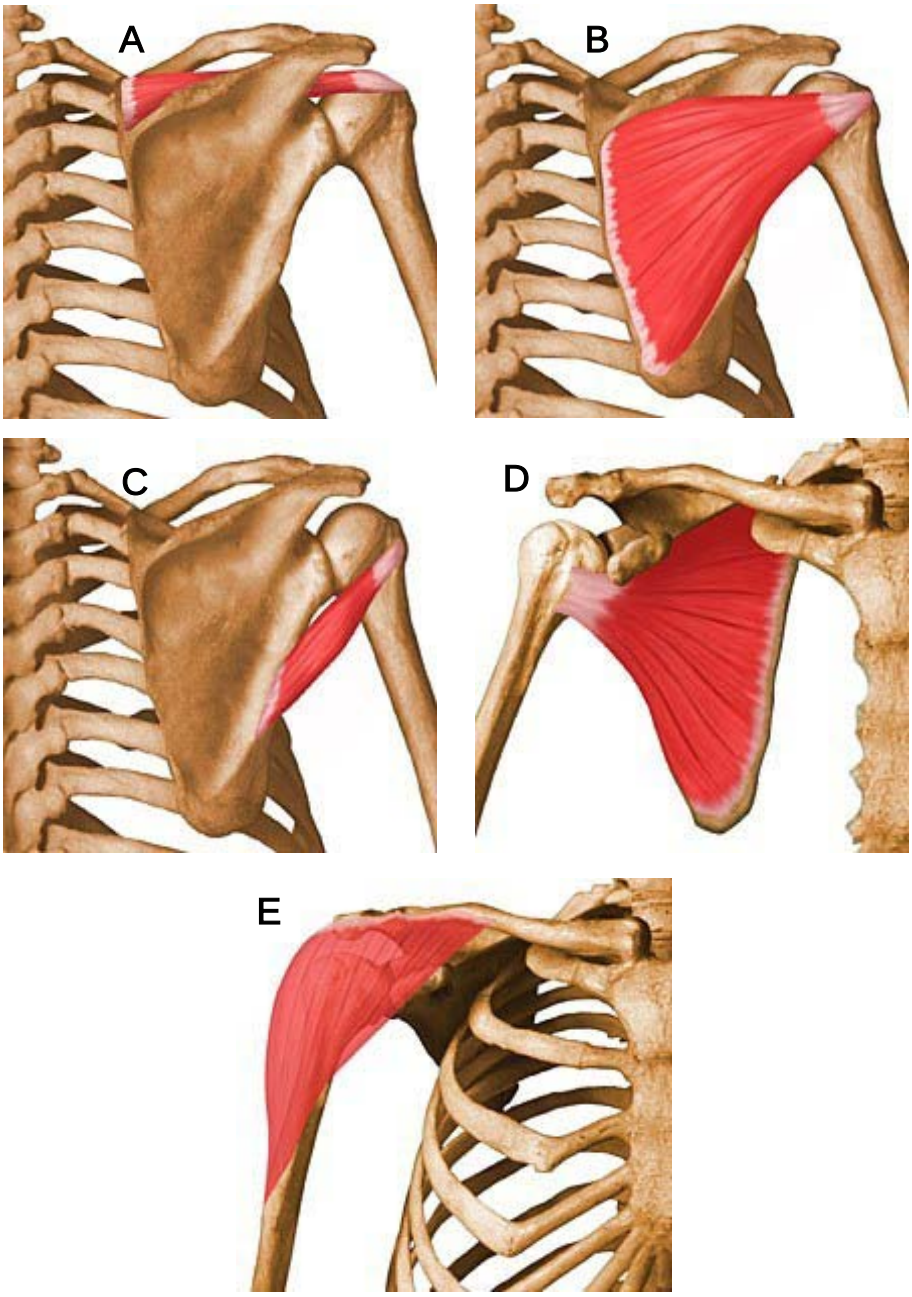

Figure 1.1 - Anatomical images of the five muscles included in the finite element model. (A)-(C) are viewed from the posterior side, (D) and (E) from the anterior side. (A) supraspinatus, (B) supraspinatus, (C) teres minor, (D) subscapularis, and (E) deltoid.

Cadaveric specimens are useful for experiments to measure the effects of forces acting on joints. Cadavers are also used to provide information for model creation and geometry[59,94,98,100]. In many experiments, a cadaveric specimen is mounted in a customized fixture which simulates a particular loading condition[52,101]. Typically, the muscle bellies are removed and thin lines are sutured to the tendons. The tendons can then be loaded dynamically[5,6], or more commonly they are loaded statically[62]. Force ratios applied to the tendon can be varied and/or supporting structures can be cut. Changes in reaction force, joint kinematics, moment arm, or other quantities can then be measured[36,78,79].

Motion capture techniques offer a way to investigate the mechanics of motion on a larger (whole limb or whole body) scale. Reflective markers can be attached to the skin and their 3D locations recorded during motion. The 3D motion of each body segment can then be calculated using inverse kinematics. This technique can be used to calculate the dynamic accelerations and moments acting on each body segment.

Recent advances in medical imaging techniques have made imaging one of the most promising tools in researching muscle mechanics[12]. Magnetic resonance imaging has been used for calculation of muscle volumes[46,91], calculation of moment arms[47,55,56,73], *in vivo* measurements of joint kinematics[34], and deformation of muscle tissue[82,116]. Ultrasound is another useful imaging modality, and can be used to dynamically track muscle fascicle motion[44,83].

Musculoskeletal models provide a powerful framework for investigating complex biomechanical systems. Computational models can be used to systematically alter input variables to determine cause and effect relationships. Computational models also afford

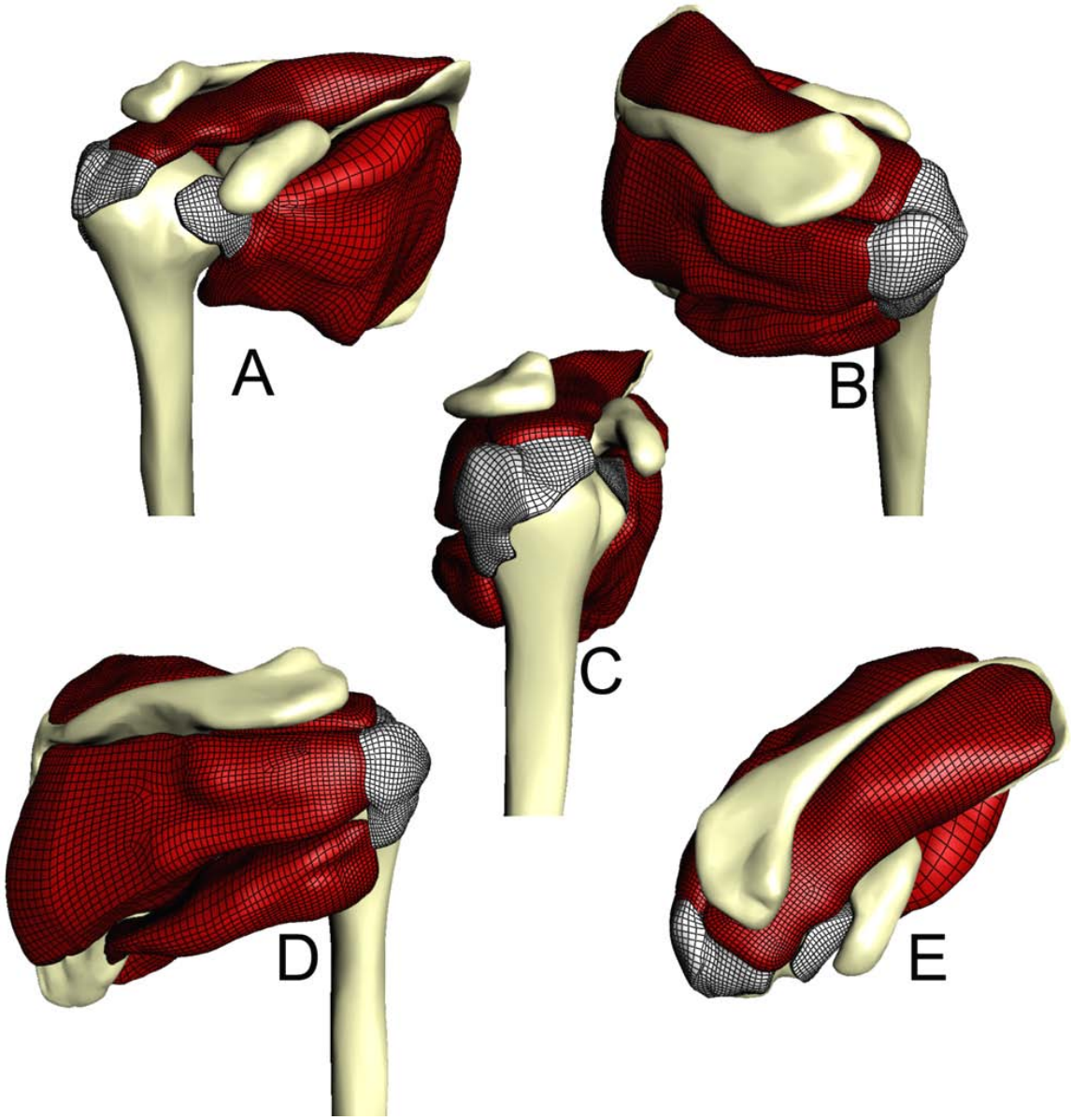

Figure 1.2 - Finite element model of the rotator cuff muscles with the deltoid removed as viewed from different perspectives. (A) anterior view, (B) superior/posterior view, (C) lateral view illustrating how cuff tendons merge together on humeral head, (D) posterior view, (E) superior view.

the opportunity to calculate parameters which are extremely difficult, or impossible to obtain experimentally. One classic example of this is the difficulty of measuring muscle forces *in vivo* under dynamic conditions. Tendon force has been measured *in vivo* by attaching a force transducer directly to the tendon[41], but this is a highly invasive experiment, and is not feasible for most joints. However, with a computational model, it is possible to simulate a dynamic motion. Then, by using mechanics and optimization, one can calculate what force each muscle must generate to produce the desired motion. Models are also advantageous for asking "what if…" questions which would not be ethical to carry out with human subjects. For example, "What if his tendon was torn? How would that change the resulting joint kinematics?" In a model this is possible, but in a living human, it is not.

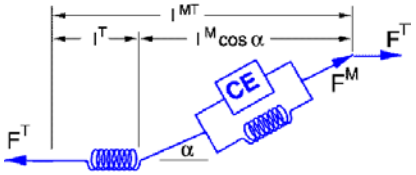

Figure 1.3 - Hill type representation of muscle

Previous shoulder models have typically modeled muscles with a collection of line segments[18,32,45,92]. These models use a Hill type muscle model[114] to represent the nonlinear force-length relationship of the muscle and tendon (Figure 1.3). A Hill muscle model approximates muscle architecture with 4 parameters; pennation angle, optimal fiber length, tendon slack length, and maximum isometric force.

Recent advances in computing speed have made it possible to investigate 3D muscle behavior using the finite element method. This method has been used successfully for skeletal muscle in a variety of applications[13-15,29,49,53,89,113]. Finite element modeling has the advantage of representing the full 3D geometry of the muscle, and efficiently

using a physics-based method of dealing with contact. However, it is computationally expensive, with even simple motions requiring long simulation times.

Shoulder models have been used to provide insight in a number of different applications, including, ergonomics[27,93], surgical simulation[86], robotics[23], control for neural prosthetics[10,11,43], wheelchair evaluation[97], and computer graphics[89]. Because line segment models are relatively simple dynamic representations of the shoulder, they can be used in conjunction with sophisticated, computationally intensive analyses such as control[11,23] and optimization[24,69,90] to better understand muscle function.

However, there are whole classes of problems which cannot be addressed by a line segment model. For instance, if one is interested in rotator cuff tears, there is no way for a line segment model to investigate the effects of partial thickness tendon tears on muscle moment arms, or the compensatory stresses generated in the surrounding muscles. Burkhart describes the geometry of several common supraspinatus tendon tears[17], but a line segment model cannot characterize the biomechanics of these types of tears, because the underlying geometry is not adequately represented.

Additionally, several characteristics of the shoulder necessitate a more detailed muscle model. First, the muscles are in constant contact with bones, and with each other. The rotator cuff muscles form a deep layer of muscle (Figure 1.2), which wraps around the glenohumeral joint. Large superficial muscles wrap over the rotator cuff, including deltoid, trapezius, and pectoralis major. Contact is difficult to represent using a line segment based approach. Interactions with surrounding tissues can be handled by defining geometric wrapping surfaces to constrain the muscle from penetrating other muscles and bones[94], or by prescribing intermediate points using a priori estimations of

the muscle path[25]. Both methods require estimating the 3D deformations of all the tissues and predicting their potential collisions and interactions. Shoulder impingement is a common shoulder injury which is related to contact[63,110]. The acromial arch forms a bony tunnel which surrounds the distal end of supraspinatus. Contact between the tendon and this arch is a pathologic condition which can be quite painful, and can lead to fraying or tearing of the cuff tendons.

A second difficulty with line segment representation of muscle is that the shoulder muscles are broad, and attach over large regions. For muscles with a small attachment region, (e.g. the short head of biceps brachii which attaches to the coracoid process), the line segment approximation seems to works well. However, the rotator cuff muscles attach over large regions of the scapula, so defining a representative muscle origin is somewhat arbitrary. Similarly, deltoid attaches over a wide length of the scapular spine and the distal third of the clavicle (Figure 1.4). Line segment models have dealt with large attachment regions by defining multiple lines of action to represent compartments of the muscle[95]. However, each line of action must use point attachments at its origin and insertion, which does not adequately constrain the rotational degrees of freedom which a broad attachment area constrains.

A third assumption made by representing muscle as line segments is that all the fibers in a muscle, or muscle compartment deform uniformly. However, imaging[82,116] and computational studies[14,15] indicate that muscle fiber strains vary in a non-uniform fashion during normal joint motions. The rotator cuff and deltoid muscles have a fan-shaped arrangement of fibers with several distinct compartments[100]. These compartments have functional implications which a simple geometric representation will not capture.

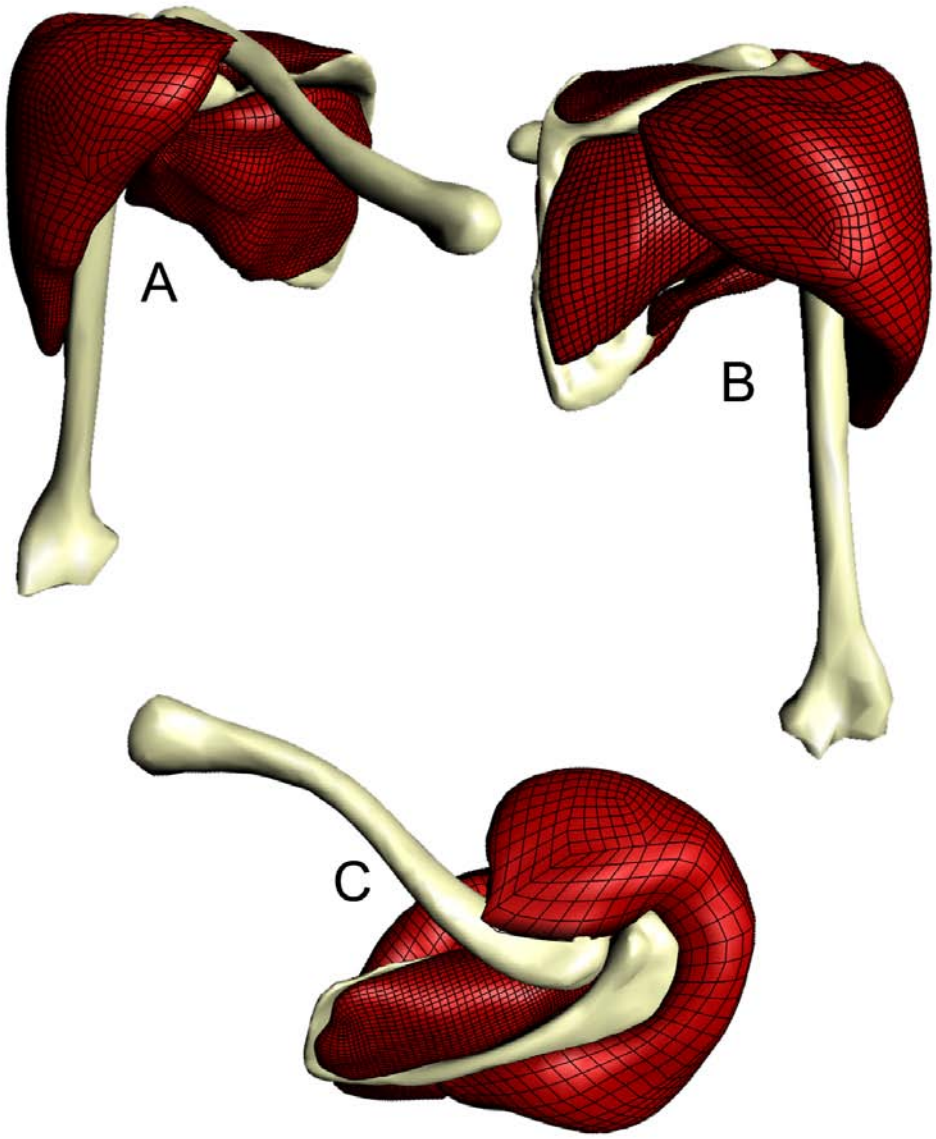

Figure 1.4 Finite element model of the rotator cuff muscles and deltoid viewed from different perspectives. (A) anterior view, (B) superior/posterior view, (C) lateral view illustrating how cuff tendons merge together on humeral head, (D) posterior view, (E) superior view.

1.1 Focus of the Dissertation

The goal of this dissertation was to investigate the functional role of the rotator cuff and deltoid muscles in actuating the shoulder. We created a 3D finite element model of normal, healthy muscles and tendons that is useful for a variety of shoulder studies. The model includes the 3D geometry of the muscles and tendons (Figure 1.3, 1.4), explicitly resolves contact between muscles and surrounding tissues, constrains muscle paths via physiologic attachment areas, and .accounts for the complicated fiber orientations within the muscles. To demonstrate the importance of 3D muscle architecture when characterizing muscle function, the model was used to calculate moment arms of the fibers through a range of joint motion.

1.2 Significance of this Research

The major contributions of this work are:

Development and testing of a finite element model of the muscles and tendons of the rotator cuff and deltoid.

An accurate, detailed 3D model of the shoulder muscles provides a powerful tool for the investigation of shoulder mechanics. In addition to improving the fidelity of moment arm calculations, and identifying muscle function, this model is ideally suited to investigate a wide range of research questions which require a detailed description of 3D geometry. Previous models with simplified geometry have many useful applications, but for investigating problems like cuff tears, and joint stability, they are insufficient. One previous 3D finite element model of shoulder muscles was developed for animation[89], but was never tested for biomechanical use. Therefore, this model is the first detailed 3D finite element model which is suitable for investigating shoulder mechanics.

Calculation of muscle fiber lines of action and moment arms for five important shoulder muscles.

This dissertation presents moment arm data for five key shoulder muscles which demonstrates how moment arms vary spatially within muscles. Moment arms characterize the mechanical function of muscle fibers, and are one of the most useful quantities for evaluating a musculoskeletal model. Moment arms from the finite element model agreed well with the range of experimental data found in the literature. This model provides a more detailed analysis of how these muscles generate motion, which will lead to better understanding of normal shoulder function.

1.3 Overview of the Dissertation

This dissertation has two subsequent chapters. Chapter 2 is written as a self-contained journal article (submitted for publication to the Annals of Biomedical Engineering with co-authors Silvia Blemker and Scott Delp) and describes the development of the finite element model of deltoid and rotator cuff muscles. The model was used to calculate moment arms using fiber paths embedded within the finite element mesh. The model was tested by comparison to published moment arm data from experiments and computational models. Chapter 3 summarizes the major contributions of this work and proposes directions for future work. The term “we” in this dissertation refers to Silvia Blemker, Scott Delp, and myself.

Chapter 2

3D finite element models of shoulder muscles for computing lines of action and moment arms

2.1 Abstract

Accurate representation of musculoskeletal geometry is needed to characterize the function of shoulder muscles. Previous computer models of shoulder muscles have represented muscle geometry as a collection of line segments, making it difficult to account for muscles with large attachment areas, muscle-muscle interactions, or complex muscle fiber trajectories typical of shoulder muscles. To overcome these issues, we developed three-dimensional (3D) finite element models of the deltoid and rotator cuff muscles to characterize muscle function. Fiber paths within the muscles were approximated, and moment arms were calculated for two ranges of motion: thoracohumeral abduction and internal/external rotation. We found that the fiber moment arms varied substantially within each muscle. For example, supraspinatus is considered a weak external rotator, but the 3D model showed the anterior fibers provide substantial internal rotation while the posterior fibers act as external rotators. Including the effects of contact, large attachment regions, and three-dimensional mechanical interactions of muscle fibers provides constraints on muscle motion, generates more realistic muscle paths, and allows for in depth study of shoulder muscle function.

2.2 Introduction

Musculoskeletal models of the shoulder typically represent muscle lines of action as a collection of line segments[32,45,92]. These models have been useful for a wide variety of applications including simulating surgical procedures[45], investigating wheelchair mechanics[93,96], and controlling neuroprostheses[11,43]. The shoulder muscles have several characteristics that make them challenging to represent using line-segment representations. Shoulder muscles have broad attachment areas, complex fiber arrangements, and paths that wrap over other muscles and bones. These important anatomical features affect muscle actions and may not be accurately characterized with line-segment approximations.

For muscles with broad attachments, a single line of action is generally insufficient to represent the geometry, so multiple lines of action must be defined[95]. This approximation makes model creation difficult because one must decide how many lines of action (i.e., compartments) to use, where to place the origin, insertion, and path of each compartment, and how to estimate the muscle and tendon parameters (e.g., optimal fiber length, maximum isometric force, *etc*.) for each compartment.

The deltoid and rotator cuff muscles have complex, fan-shaped arrangement of fibers and multiple functional compartments.[100] It is possible to represent multiple compartments of a muscle with separate lines of action, but line segment models assume that all fibers within a functional compartment deform uniformly and independently of neighboring compartments. Imaging[12,82,116] and computational studies[14,15,28,112] have demonstrated that deformations can be non-uniform within muscles, and biomechanical

experiments have demonstrated that adjacent muscle compartments are not mechanically independent[48,50,72].

Shoulder muscles wrap over each other and other surrounding tissues; therefore, to accurately represent shoulder muscle geometry, it is important to model muscle-muscle and muscle-bone interactions. For line segment models, geometrical constraints, such as "via points" or wrapping surfaces[13], are used to represent contact with surrounding tissues and approximate the resulting muscle paths. Prescribing these geometrical constraints is challenging because it requires knowledge of how the muscles deform in three dimensions.

Three-dimensional (3D) finite element (FE) modeling allows representations of muscles with broad attachment regions, incorporation of complex fiber trajectories, and modeling of contact between muscles and surrounding structures based on their physical interactions[13,30,65,71,80]. The goals of this study were to: *(i)* develop and test 3D finite element models of the deltoid and rotator cuff muscles and tendons to investigate how moment arms vary across the fibers within each muscle, and *(ii)* compare the 3D models with line-segment representations to characterize how predictions of shoulder muscle moment arms differ when the complexities of broad attachment areas, complex fiber arrangements, and wrapping are explicitly modeled.

2.3 Methods

The 3D models of the shoulder muscles were constructed from magnetic resonance imaging (MRI) of a single healthy subject. The MR images were segmented to define the anatomical structures and a finite element mesh was fit to each structure. Bones were represented as rigid bodies. Muscles and tendons were represented using a

nearly incompressible, hyperelastic, transversely-isotropic constitutive model[13]. Fiber maps that represent the three-dimensional (3D) trajectories of the fibers were constructed for each muscle[13]. The kinematics for shoulder abduction and shoulder rotation were prescribed as input to the finite-element simulations and the resulting muscle deformations were predicted. The fiber deformations were tracked through the finite element solution, and a moment arm was calculated for each fiber at each joint angle. Analysis of the fiber moment arms provided insights into the function of the muscles.

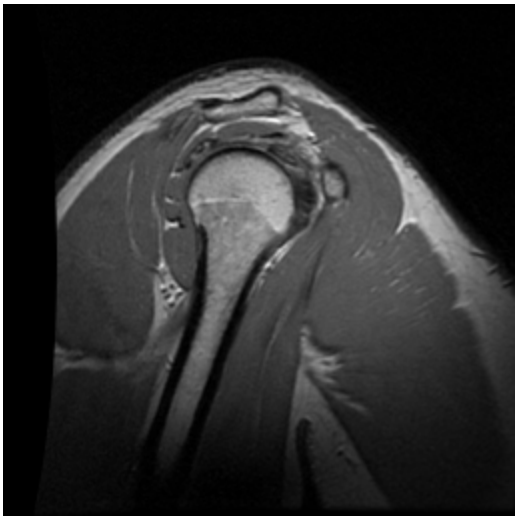

Figure 2.1 - Fast Spin Echo MR image of the rotator cuff. Image is of the right shoulder and is viewed in the sagittal oblique plane. The right side of the image is the anterior side of the shoulder.

2.3.1 Imaging and Geometry

The 26-year-old male subject with no history of shoulder pathologies or injuries (height: 1.75 m, weight: 80 kg) provided informed consent, in accordance with the Institutional Review Board at Stanford University, and was imaged in a supine position with arms at his sides in a 1.5 T MRI scanner (GE Healthcare, Milwaukee, WI) using a body coil. Image parameters were chosen to maximize the contrast at muscle boundaries. We used two imaging protocols, one for the rotator cuff and another for the deltoid and bones. The rotator cuff was imaged using a sagittal oblique imaging plane (Figure 2.1) and a 2D Fast Spin Echo (2D FSE-XL) sequence (20 cm x 20 cm field of view, 2.5 mm

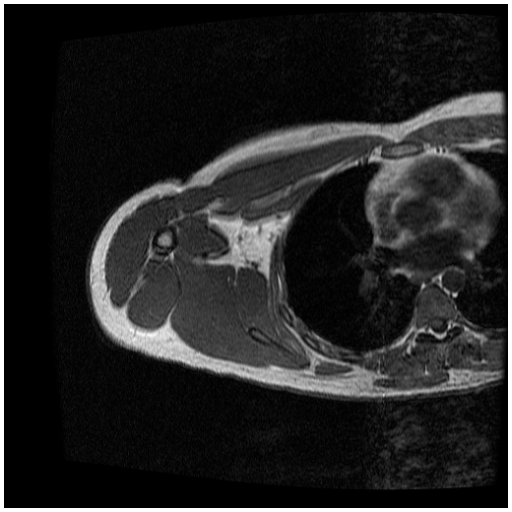

Figure 2.2 - Axial Spoiled Gradient MR image of the right shoulder. The imaging plane in this image goes through the axilla and the heart. This image sequence was used to create the deltoid, and humerus models.

slice thickness, 1 mm space between slices, TR 4200 ms, TE 13.4 ms, in plane resolution 0.78 mm, flip angle 90°). This series ranged from the lateral edge of the shoulder to the medial border of the scapula. The deltoid and bones were imaged using an axial image plane (Figure 2.2). A 3D Spoiled Gradient (3D SPGR) sequence was used for this series (40 cm x 40 cm field of view, 3 mm slice thickness, TR 11.64 ms, TE 5.3 ms, in plane resolution 0.78 mm, flip angle 30°). This series ranged from approximately the fourth cervical vertebra to the distal end of the humerus. Surfaces of the muscles, tendons, and bones were defined by manually outlining the boundaries of each tissue on each image (3D Doctor, Able Software, Lexington, MA). These outlines were used to create 3D surfaces representing the anatomical structures. The surfaces were imported into Truegrid (XYZ Scientific, Livermore, CA), a finite element mesh generator. A finite element mesh was constructed for each muscle-tendon unit (Figure 2.3). Muscle and tendon geometry were represented with eight-node, linear hexahedral elements, and bone surfaces were represented as rigid linear triangular surface elements (Table 2.1).

In order to define the three-dimensional trajectories of fibers within each 3D muscle model, we used a mapping technique that applies a specific muscle architecture to the FE mesh, as described in Blemker and Delp.[13] For the shoulder models in this study,

we applied the “fan-shaped” architecture to each muscle mesh. For each muscle, the fiber mapping was defined such that the fibers originated along the proximal tendons and inserted along the distal tendons (Figure 2.4), in accordance with photographs taken from dissected shoulder muscles. The trajectories and regions of fibers in the model qualitatively agreed with those described by Ward et al.[100] and Kim et al.[58] Based on the fiber trajectories, a fiber direction vector was determined for each element in the mesh to serve as an input to the constitutive model.

Table 2.1: Summary of the nodes and elements in the finite element model

Muscle	Nodes	Elements	# tendon branches
Supraspinatus	26138	23610	1
Infraspinatus	21320	19119	3
Teres Minor	14358	12848	2
Subscapularis	20091	17899	6
Deltoid	15972	14088	0
Bones	7436	14860	NA
Total	105315	87564	NA

2.3.2 Constitutive Model

We used a nearly-incompressible, hyperelastic, transversely-isotropic constitutive model[13,20,105] to characterize the non-linear stress-strain relationship of muscle and tendon. This constitutive model characterizes the active and passive behavior of muscle along the direction of muscle fibers based on the force length relationship of a sarcomere[114], with a specified activation level between 0 and 1. The model also includes the contributions of strain energy for shear deformations both in the plane transverse to fibers and between adjacent fibers. Tendons were modeled with the same material model,

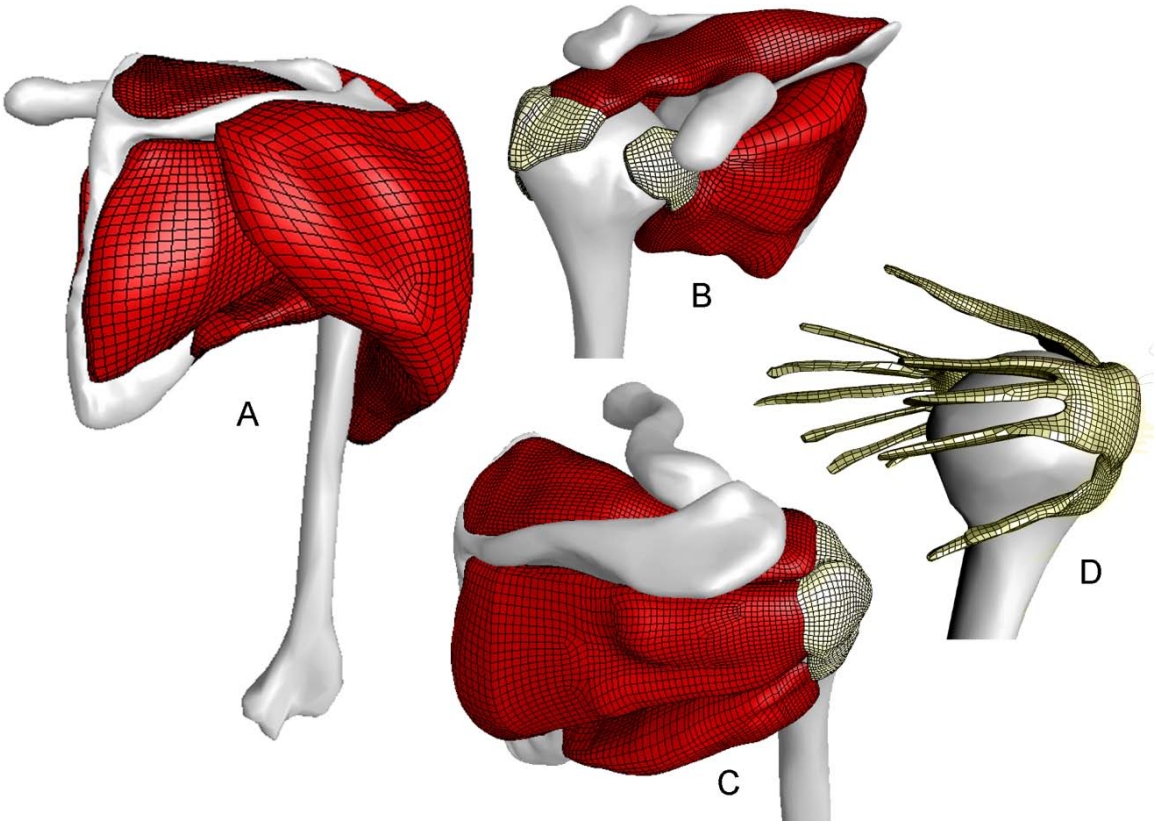

Figure 2.3 - Finite element model of the shoulder musculoskeletal system. Muscles are shown in red, bones in white, and tendons in yellow. (A) Posterior view illustrating the models of the deltoid and rotator cuff muscles. (B) Anterior view of the rotator cuff with the deltoid and clavicle removed illustrating subscapularis and supraspinatus. (C) Posterior view of the rotator cuff with the deltoid removed illustrating infraspinatus and teres minor. (D) Posterior view of rotator cuff tendons attached to the humeral head.

but have different parameters which describe their along-fiber and cross-fiber properties. For tendon, the fiber force response is exponential, and the shear modulii are 100 times stiffer than muscle. A thorough description of the constitutive model can be found in Blemker et al.[6]

2.3.3 Finite Element Simulations and Computation of Fiber Moment Arms

The three rotations of the humerus were prescribed, where the motions of the scapula and clavicle were determined based on published regression equations.[22] The glenohumeral joint was represented as a ball-and-socket joint, and the rotation center was determined by fitting a sphere to the articulating surface of the humeral head[75,94]. Bony landmarks were digitized and bone axes were defined in accordance with the recommendations of the International Society of Biomechanics[22,108].

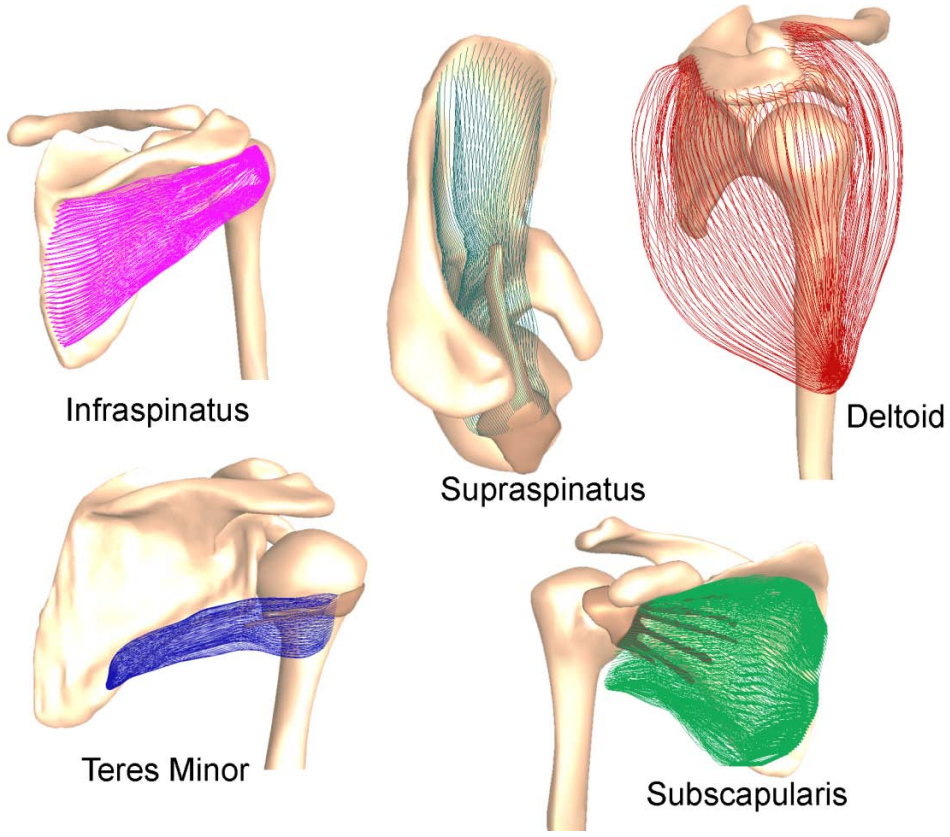

Figure 2.4 - Three-dimensional fiber trajectories for each of the shoulder muscles

We simulated two motions of the shoulder. The first motion ranged from 0 to 90 degrees of thoracohumeral abduction. The second motion ranged from 45° of internal rotation to 45° of external rotation, where the abduction angle was fixed at 0°. In order to analyze each muscle's action for each of these motions, we prescribed each of the two motions (in one-degree increments) while applying a moderate level of activation for each muscle (0.1-0.3 for abduction, 0.02-0.12 for rotation). Finite element simulations were run using Nike3D, an implicit finite element solver[85] on a Workstation (Dell, dual quad-core Xeon processor, 20Gb RAM) and took approximately 12-20 hours.

We sampled the fiber maps (defined above) for each muscle to obtain evenly distributed representative fibers that we could track throughout a simulation. The length of each fiber was then calculated as a function of thoracohumeral angle. The moment arm for each muscle fiber was determined using the principle of virtual work:[4,47] $ma_f = \frac{\partial l_f}{\partial \theta}$, where ∂l_f is the change in length of the muscle fiber and $\partial \theta$ is the change in thoracohumeral angle. Differentiation was performed using a second order central difference algorithm, and the moment arms were then smoothed using a second order, low-pass Butterworth filter with a cutoff frequency of 1 rad^{-1}. We compared the fiber moment arms predicted by the 3D models with moment arms determined experimentally[2,33,61,68,81] and from a published model of the upper extremity (with series of line segment representations of muscle)[45].

2.4 Results

2.4.1 Abduction Moment Arms

The abduction moment arms of the muscle fibers within each muscle vary substantially (Figure 2.5). Supraspinatus fiber moment arms range from 1.0 cm to 2.0 cm at neutral position (0° abduction) and from 0.3 to 1.0 cm at 90° of abduction (Figure 2.5A). The model of the upper extremity that uses a series of line segments[45] for this muscle has a moment arm similar in magnitude to the 3D model, but that changes more with shoulder abduction angle. The abduction moment arm is nearly zero in the line segment model when the shoulder is abducted, but the finite element model reveals that the moment arm is maintained with abduction.

Infraspinatus moment arms vary from 1.2 cm adduction to 1.3 cm abduction at 0° of abduction (Figure 2.5B). The fibers with adduction moment arms are located on the inferior portion of the muscle, near teres minor. The line segment-based model[45] predicts that infraspinatus is a weak abductor, while the 3D model predicts that the superior fibers of the muscle are strong abductors, whereas the inferior fibers are adductors.

Teres minor moment arms vary from 0.0 to 1.4 cm of adduction (Figure 2.5C). Teres minor fibers have a nearly constant adduction moment arm throughout the range of motion, which is consistent with its insertion on the inferior part of the greater tubercle, below the rotation center of the humeral head. Teres minor has the smallest cross section and the most parallel fibers of these muscles, and thus it agrees well with a line segment representation[45,81].

Subscapularis moment arms vary from 1.7 cm adduction to 1.0 cm abduction at the neutral position (Figure 2.5D). Abduction moment arms for the subscapularis

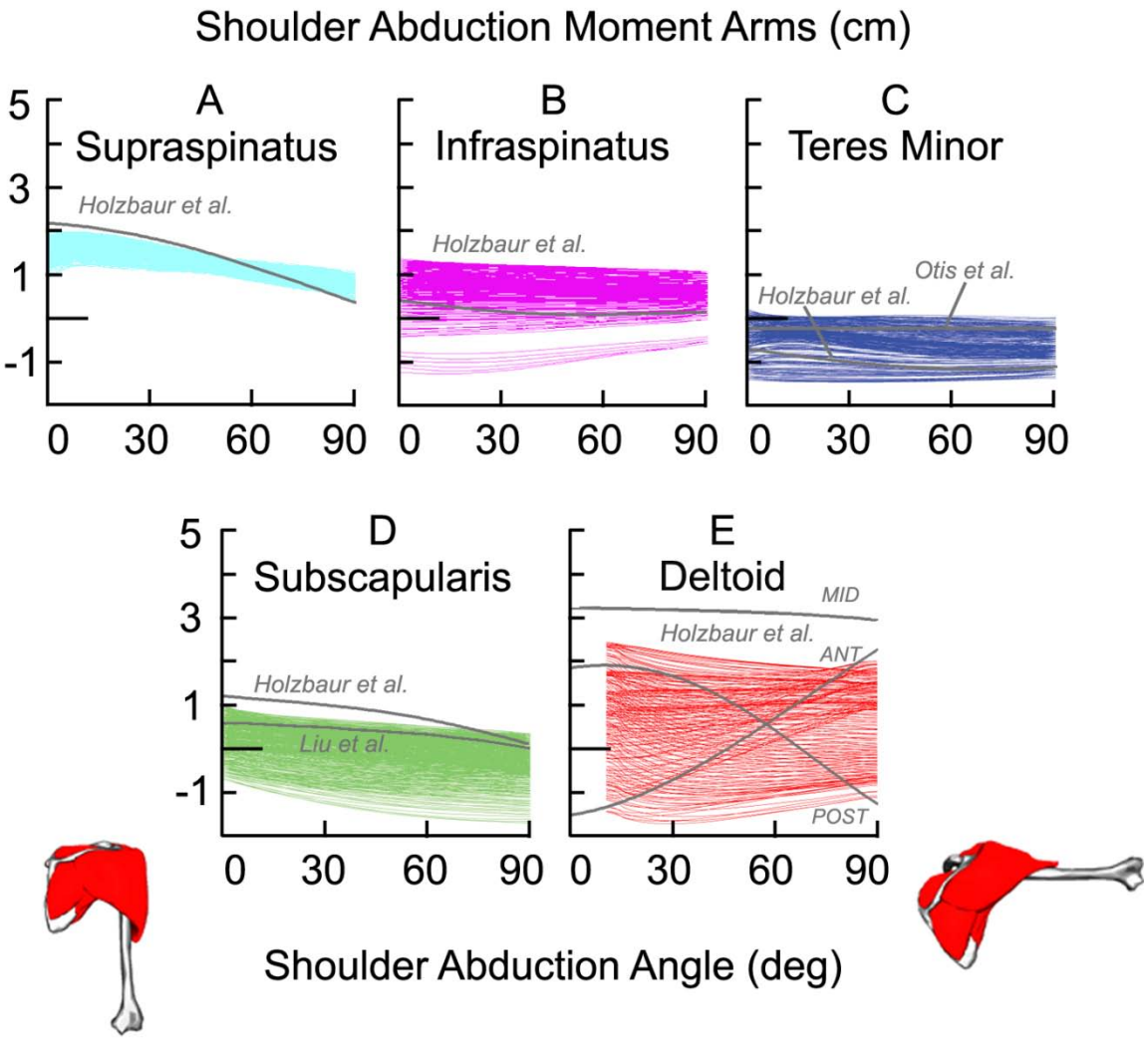

Figure 2.5 – Shoulder abduction moment arms for each fiber in the finite element model of the supraspinatus (A), infraspinatus (B), teres minor (C), subscapularis (D), and deltoid (E) over a range of shoulder abduction angles. Abduction moment arms are positive. Moment arms computed with the model of Holzbaur et al.[45], and experimental measurements by Liu et al.[68], and Otis et al.[81] are shown for comparison. The moment arms from Liu et al.[68] are scaled by two-thirds because they were reported as a function of glenohumeral, rather than thoracohumeral angle, and Inman et al.[51] reported a 2:3 ratio of glenohumeral to thoracohumeral angle. ANT, MID, and POST in E designate the anterior, middle, and posterior lines of action from Holzbaur et al.[45]

decrease with abduction angle. The superior fibers of subscapularis are abductors, while the middle and inferior fibers are adductors. The line segment model[45] and experimental data[68] predict that the muscle is a weak abductor, while the 3D model suggests that a large portion of the muscle contributes to adduction.

Deltoid abduction moment arms range from 2.5 cm abduction to 1.2 cm adduction (Figure 2.5E). The fibers in the middle compartment have the largest abduction moment arms, while the fibers at the anterior and posterior borders have adduction moment arms. The 3D model agrees well with the experimental findings of Liu et al.[68] The abduction fiber moment arms in the 3D model remain relatively constant with abduction angle, but the three-line segment approximation of deltoid[45] (Figure 2.5E, grey lines) predicts that the anterior and posterior deltoid have moment arms that vary greatly with abduction angle.

2.4.2 Rotation Moment Arms at 0 Degrees of Thoracohumeral Abduction

Supraspinatus rotation moment arms range from 1.5 cm internal to 0.5 cm external rotation at 45° of internal rotation, and from 1.2 cm internal to 1.8 cm external rotation at 45° of external rotation (Figure 2.6A). Anterior fibers remain internal rotators, and posterior fibers remain external rotators throughout the range of motion. The fibers increase their external rotation potential as the 3D model moves into externally rotated positions.

Infraspinatus moment arms range from 0.2 cm internal to 1.7 cm external rotation at 45° of internal rotation, and from 0.2 to 2.5 cm external rotation at 45° of external rotation (Figure 2.6B). External rotation moment arms increase with external rotation angle, giving infraspinatus better leverage in externally rotated positions. The line segment model[45] predicts an external rotation moment arm as large as the largest moment arm in the 3D model.

Teres minor moment arms vary from 0.5 to 2.2 cm external rotation (Figure 2.6C). The fibers of teres minor function as external rotators throughout the range of

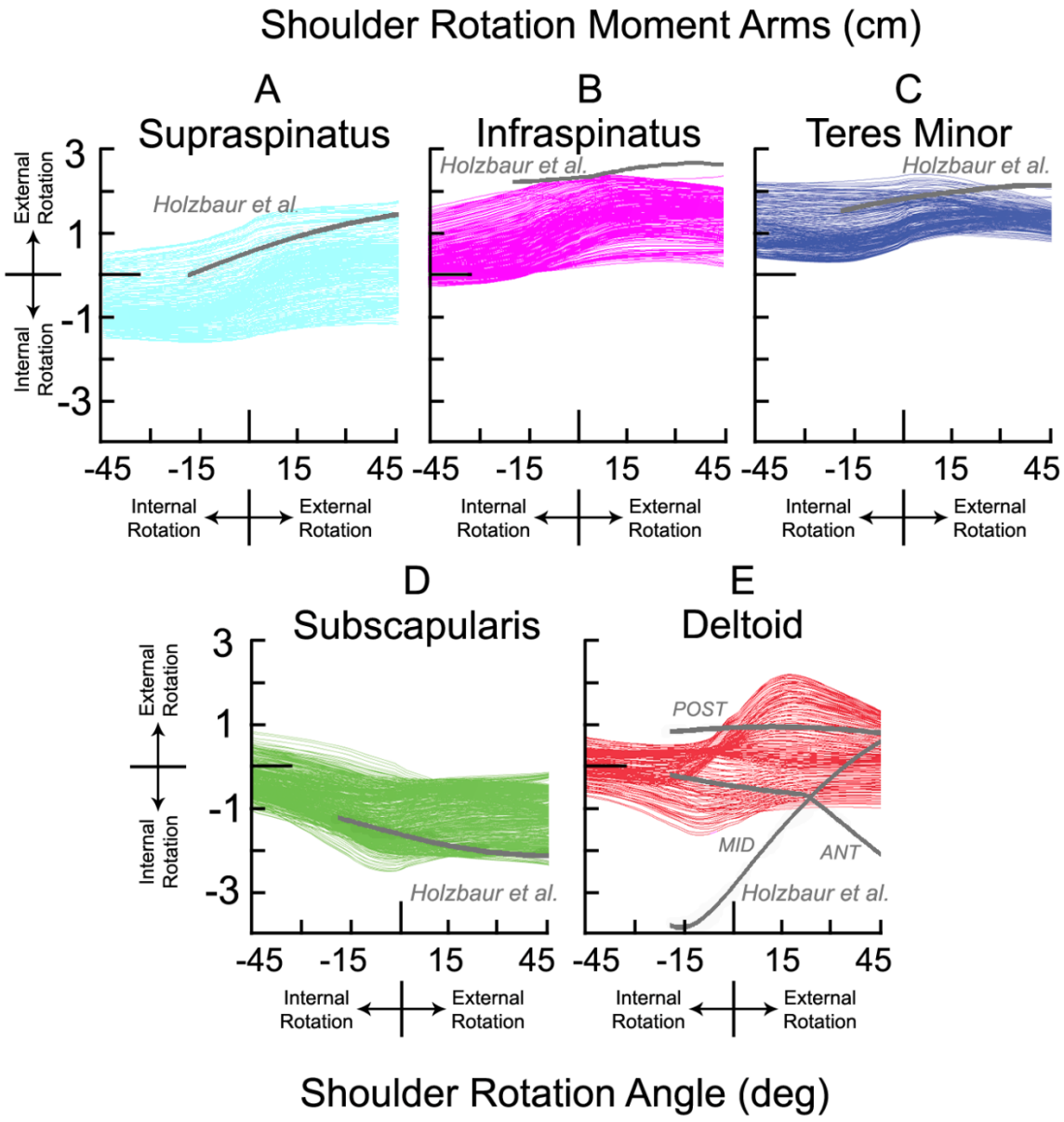

Figure 2.6 - Rotation moment arms for muscle fibers in the finite element model. Rotation occurs at 0° of abduction. Gray lines are moment arms calculated by the Holzbaur line segment model[45]

motion and slightly increase their external rotation moment arms as the shoulder externally rotates. The rotational action of teres minor is represented well by a line segment approximation[45].

Subscapularis moment arms vary from 1.0 cm internal to 0.8 cm external rotation at 45° of internal rotation and 0.3 to 2.5 cm internal rotation at 45° of external rotation

(Figure 2.6D). The subscapularis moment arms become more internal with external rotation angle. While most the subscapularis fibers act as internal rotators, a few fibers act as external rotators at internally rotated positions. The moment arms calculated by the line segment model are close to the fibers with the greatest internal rotation fiber moment arm from the 3D model.

At internally rotated positions, the rotation moment arms of the deltoid range from 0.75 cm internal to 0.75 cm external rotation (Figure 2.6E). As the arm moves into external rotation, the external rotation moment arms of the posterior deltoid fibers increase while the internal rotation moment arms of the anterior fibers remain nearly constant. The posterior deltoid line of action of the three-line-segment model agrees well with the posterior fibers of the 3D model. However, the moment arms of the middle and anterior lines in the line segment model vary much more with shoulder rotation angle than those predicted by the 3D model.

2.5 Discussion

We compared 3D finite element models of shoulder muscles to line segment models of the same muscles. Overall, there was reasonably good agreement between the 3D models and line segment models, with two important exceptions. First, the line segment models under constrained the muscle paths in some cases; therefore, line segment based moment arms changed more with joint rotation than moment arms predicted by the 3D models. Second, the 3D models predicted substantial variability in moment arms across fibers within each muscle, which is not generally represented in line segment models.

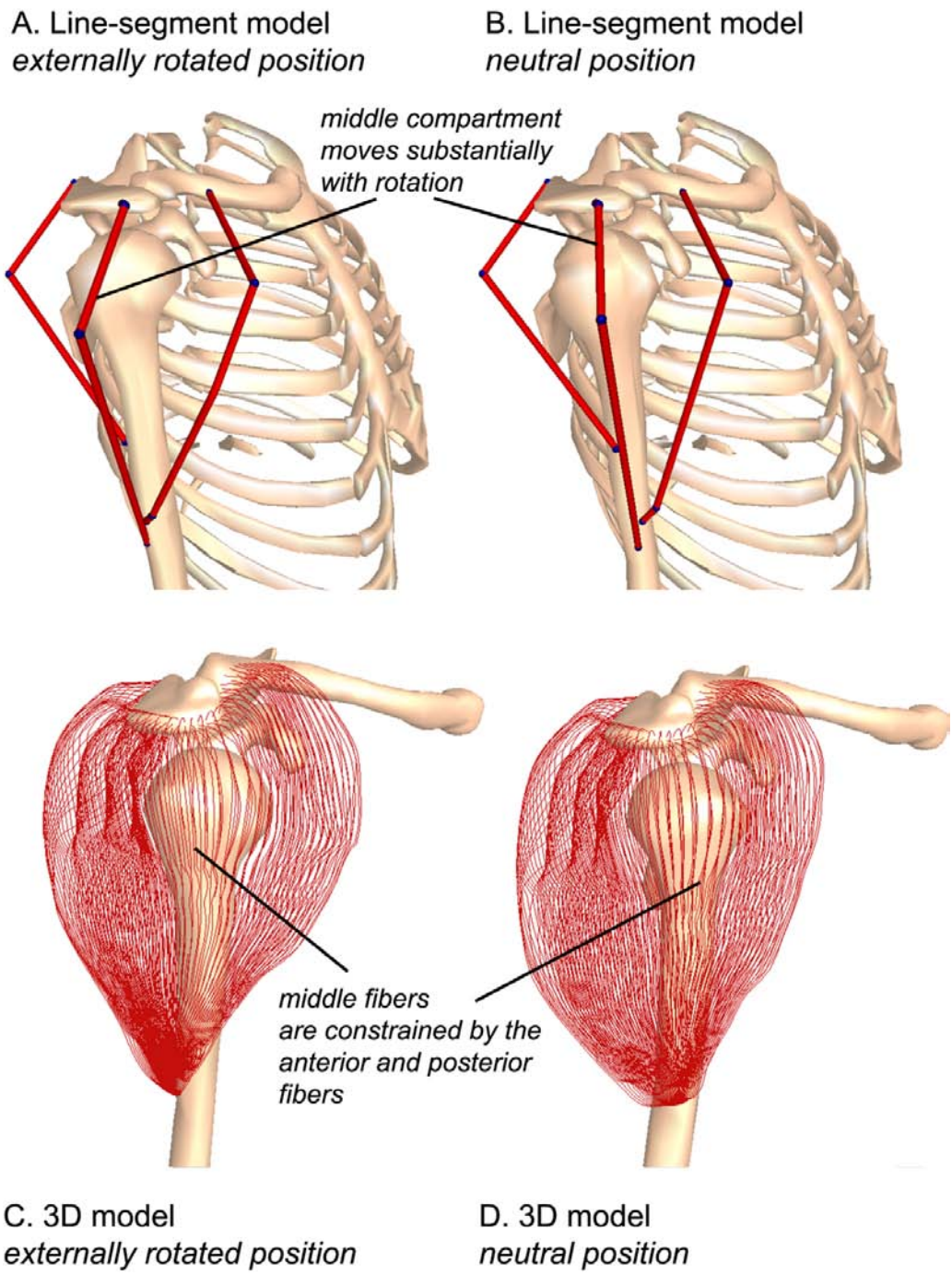

Figure 2.7 - Comparison of muscle paths for a line segment model of the deltoid (A,B) and the 3D finite element model of the deltoid (C,D) over a range of shoulder rotation (45° external rotation (A,C) to neutral (B,D)). When the humerus is externally rotated, the middle compartment of the line segment model slides posteriorly. In contrast, the 3D muscle model fibers slide only slightly between the two positions, due to the constraints associated with the mechanical interaction between compartments and preservation of muscle volume.

The issue that line segment models under-constrain muscle paths was most noted in the deltoid, where the muscle is separated into three separate compartments. When line segment models separate muscles into multiple compartments, the compartments are assumed to be mechanically independent, and therefore their paths can move freely with respect to one another. As an illustration (Figure 2.7), a comparison of the line segment deltoid model and the 3D deltoid model demonstrates how, in the 3D model, the motions of the middle fibers are constrained by the interactions with the neighboring muscle tissue, whereas in the line segment model the middle compartment path moves freely without constraints. While, theoretically, via points of a line segment model could be defined to represent these constraints, it is extremely difficult to define how these interactions constrain the path for all of the feasible motions of shoulder.

Muscle fiber moment arms were found to vary substantially within each of the shoulder muscles studied, for some muscles by more than 100% of the mean moment arm. This variation occurs because the rotator cuff muscles have fibers that span the joint (in contrast to other muscles in which the tendons span the joint). The high degree of variability in moment arms across fibers could have important implications on the force generating capacity of these muscles, because variable fiber excursions suggest that the fibers are operating on different regions of the force-length curve. Variable fiber moment arms also indicates that strains are nonuniform within these muscles during joint motions, which has been demonstrated in a previous imaging study of the rotator cuff[116] and may have important implications on rotator cuff injury mechanics.

Contact and wrapping play a critical role in shoulder muscle deformations, which affect moment arm calculations. While line segment models have the capability of

interacting with wrapping surfaces that capture the effect of underlying structures, discontinuities in moment arm predictions often occur when the lines of action intersects with the wrapping surface (for example the anterior fibers of the deltoid in external rotation, Figure 2.6E). The 3D models allow for smooth representation of contact between muscles, tendons, and bones, without the need for prescription of via points or wrapping surfaces.

While using 3D finite-element models of shoulder muscles yields higher fidelity muscle paths, the extra detail comes at the cost of high computation times. The finite element model can take up to 20 hours to simulate simple motions. In contrast, line segment models can be controlled in real time, which is important for time-sensitive applications such as neuroprosthetic control[10]. Halloran et al.[38,39] developed a surrogate modeling approach that allows for efficient concurrent simulation of finite element foot models and forward dynamic models of movement. Extension of these types of techniques to handling 3D finite element muscle models would expand the impact and applicability of the 3D shoulder muscle models described here.

Three-dimensional muscle models require more input data than line segment models. For example, the 3D models require specification of the spatial distribution of fiber directions across the muscle mesh. To provide a detailed description of the fiber directions, we used a mapping method that incorporates knowledge of each muscle's architecture, along with specification of the areas of fiber origin and insertion. Our fiber maps are in good agreement with measurements by Ward et al.[100] and Kim et al.[58] In the future, refinements of diffusion tensor MRI techniques[31,77,84] may enable characterization

of the shoulder muscles and would provide *in vivo* measurements of fiber trajectories to be used in 3D models.

The results presented in this study are based on a model of one subject. To develop a model that was representative of normal, healthy shoulders, we opted to use imaging data from an average sized, healthy young adult. Previous shoulder models have typically been derived from either the visible human project[10,11,19,32,89,111] or cadaveric data[45,46,92]. The visible human subject was large and highly muscular, whereas cadaveric specimens often suffer from atrophy. Therefore, one would expect that some of the differences between our results with other data would be due to these different subject populations. Gatti et al.[33] compared abduction moment arms from seven different experimental studies and six different models, all from different subject populations. It is interesting to note that the range of reported abduction moment arms for each muscle (roughly 1 to 2 cm range across all the studies) was similar to the amount of variation in moment arms across the fibers of each of our 3D muscle models. This suggests that the variation observed across studies could at least in part be explained by differences in the regions of the muscles that are represented in each study.

The 3D finite element shoulder models described here provide highly realistic representations of shoulder muscle lines of action, and they allowed for insights into the effects of contact, broad attachment, and complex fiber arrangements on shoulder muscle actions. Although line segment models well represent muscle geometry in some positions, they do not represent the variation in moment arms across fibers, nor do they accurately reflect the effects of mechanical coupling between muscle compartments on

muscle path motion. This study has demonstrated the potential for using 3D models to capture the complex 3D mechanical function of shoulder muscles.

Chapter 3

Conclusions and Future Work

The purpose of this dissertation was to investigate the role of the rotator cuff and deltoid muscles in mobilizing the shoulder. Previous shoulder models have used simplified muscle geometry, and have not considered the impact of complex geometry and fiber trajectories within muscles on moment arm and joint stability calculations. We developed a 3D finite element model of five important shoulder muscles, and calculated moment arms of the muscle fibers for shoulder abduction and rotation. The moment arms from the finite element model agreed well with experimental measurements and revealed that muscle deformation is not uniform within these muscles. Moment arms varied across the muscles, indicating that different regions of the same muscle can simultaneously have different mechanical functions.

3.1 Contributions

The main contributions of this dissertation are:

The creation and testing of a finite element model of the rotator cuff and deltoid

This shoulder model faithfully represents the 3D geometry of the muscles of a healthy shoulder, and is to our knowledge, the first 3D finite element model for characterizing shoulder function. The best kinematic data available was used to implement the shoulder rhythm[22]. The model accurately reproduces the complex geometry of the muscles and tendons. It represents the 3D variation of fiber orientations within the muscles and physically resolves interactions between contacting surfaces. The model was tested by comparing moment arms with published data. This model should

serve as a valuable tool for furthering our understanding of shoulder mechanics, both in normal and pathological cases. There are several additional applications for which this model will be used, which are discussed in more detail in Section 3.2.2.

Calculation of muscle fiber lines of action and moment arms for five important shoulder muscles

Much attention has been given in the literature to the calculation of moment arms and muscle paths. Moment arms are perhaps the single most important parameter in a musculoskeletal model because they characterize muscle function and muscle paths. This model provides the ability to calculate, with a high level of detail, the moment arms of these important shoulder motions while typical simplifications to muscle paths were carefully avoided. With the finite element model we discovered that the common practice of defining multiple lines of action to represent broad muscles generally leads to a much larger change in moment arms with joint rotation than the finite element model would indicate.

3.2 Future Work

There are many potential applications of the research described in this dissertation. Several of these are outlined below.

3.2.1 Additional applications of the finite element model

Contributions of the deltoid and rotator cuff to glenohumeral stability

Shoulder instability is common and is difficult to treat and diagnose[1]. Anterior and inferior instability are the most common directions, accounting for over 90% of cases (ref). As discussed in chapter 1, the recurrence rate of shoulder dislocations is high[99], treatments fail to restore function in many cases[103], and surgery may have side effects including motion loss[26,78] and joint degeneration[1,26,78]. Muscles have been shown to be a primary source of stability throughout the range of motion[62,64,74]. Kido et al.[57] found that as the passive stabilizing structures were damaged (i.e., capsule, ligament, labrum), the muscles became more effective at joint stabilization. Previous studies on muscle contribution to shoulder stability have generally used a line segment representation of muscle paths, calculated a resultant joint force, resolved this vector into compression and shear components, and calculated a stability ratio[3,64,111]. However, we hypothesized that the simplified geometry of line segment representations may miss important mechanisms of stability. To test this hypothesis, we used the 3D finite element model described in this dissertation to characterize how muscles stabilize the shoulder by resisting glenohumeral joint translation.

We simulated four glenohumeral translations, each corresponding to a common clinical exam for instability. One cm translations of the humeral head were imposed in

the anterior and inferior directions (with respect to the glenoid) with the arm in two positions; neutral (0° abduction) and abducted 90° in the scapular plane. Fiber motion was tracked through the finite element solution to determine the change in length of muscle fibers with joint translation. To quantify muscle contributions to stability we introduced a novel metric, the fiber stability index. It is defined as $FSI_f = \frac{\partial l_f}{\partial x}$ where ∂l_f is the change in length of the muscle fiber and ∂x is a specified joint translation. The fiber stability index is derived from the principle of virtual work, accounts for pennation angle, and represents the mechanical advantage a muscle fiber has to resist or encourage joint translation. If a fiber lengthens with joint translation, it is a stabilizer because active contraction of the muscle fiber would cause the muscle fiber to shorten, and would generate a force to resist translation. A negative FSI indicates that a fiber shortened for a given translation, and active contraction of this muscle fiber would generate a force to encourage translation.

At neutral position with an anterior translation, (representing the load shift clinical exam), we found that the deltoid is the strongest stabilizer (Figure 3.1), with the anterior deltoid providing the most stability, and the posterior deltoid providing the least. This disagrees with previous stability analyses which found anterior deltoid to be an anterior destabilizer[62]. When the arm is abducted to 90° and the humeral head is translated anteriorly (representing the anterior drawer exam), all the FSI decrease, and the anterior deltoid becomes the most destabilizing muscle while the middle and posterior deltoid, along with posterior supraspinatus, provide the most stability. This agrees with previous assessments of stability[62]. For inferior translation, the deltoid and supraspinatus had large FSI at both joint angles.

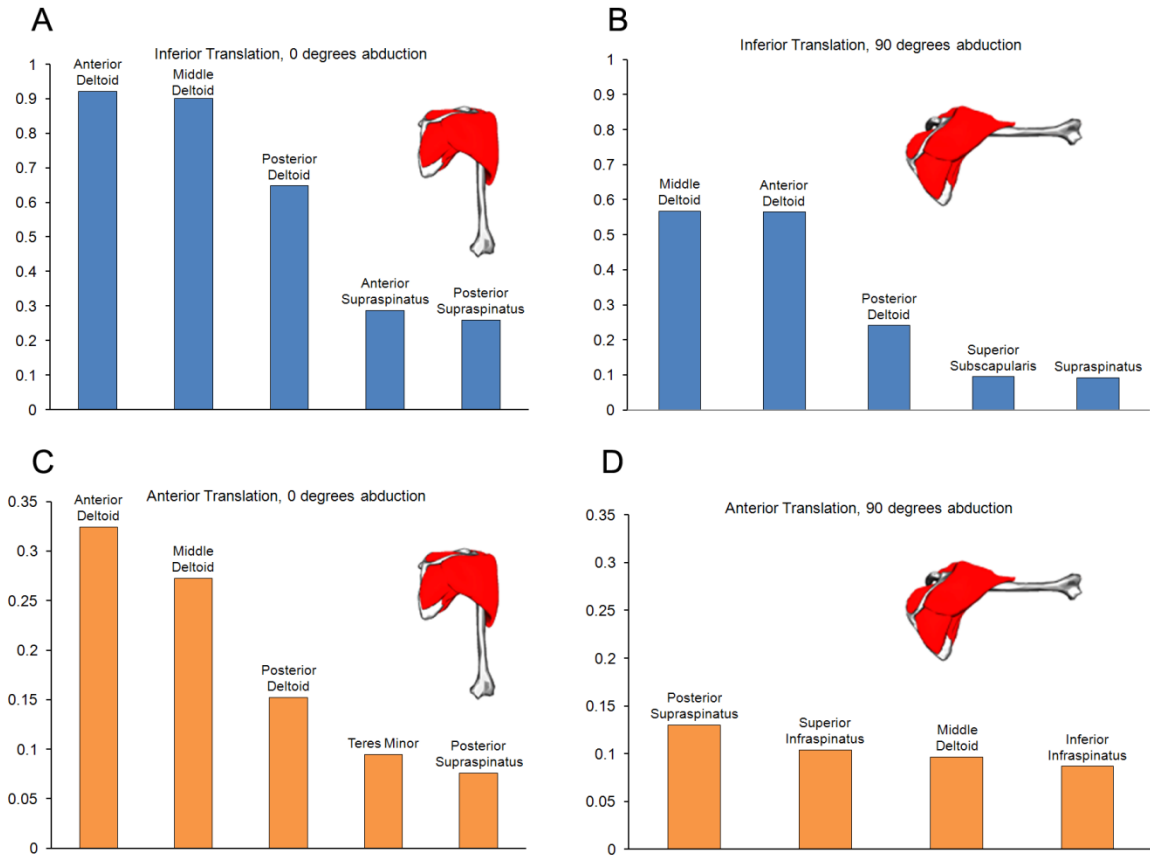

Figure 3.1 – Largest average fiber stability indices (FSI). Large FSI indicates a strong stabilizer which resists translation for (A) inferior translation, 0° abduction, (B) inferior translation, 90° abduction, (C) anterior translation, 0° abduction, (D) anterior translation, 90° abduction

Previous studies have ignored the fact that muscles not only generate tensile forces, but they also wrap over each other, and the underlying bones. When the humeral head is translated anteriorly into the deep fibers of the anterior deltoid, the fibers are oriented to generate an anterior force, but they are stretched by contact with the humeral head. Therefore, in this case, the anterior deltoid provides stability, not from its effective line of action, but from compressive forces generated by muscle-bone contact. When the arm is abducted, the humeral head rotates out from under the deltoid, and stability is

characterized more from fiber orientations than contact, which agrees with line segment predictions.

This study demonstrated that the finite element model presented in this dissertation can be used to provide new insight into the way that these muscles function to dynamically stabilize the shoulder. By including contact, and 3D geometry, we were able to use the model to identify a mechanism of joint stability that has not been previously reported.

Simulate common rotator cuff tears

Rotator cuff tears are a common and intriguing shoulder pathology. Often, a cuff tear is a debilitating injury, yet imaging studies have revealed that a large proportion (23%) of elderly adults have asymptomatic cuff tears[88]. Some people function well for many years with a cuff tear, while others, having a similar tear (size, shape, and location), lose overhead functionality of the arm. It is not known what factors make a tear symptomatic or asymptomatic, but the model we have developed allows for systematic investigation of the underlying mechanics. The vast majority of tears start in the supraspinatus tendon, and as they progress, they spread to the infraspinatus and teres minor. The size, shape, and location of these tears has been well documented in the surgical literature[16,17]. Since we have now defined moment arms and fiber stability indices for a normal shoulder, we can do a direct comparison to see what changes would occur if the tendons were torn. The resulting increases in stress in the unaffected muscles, as well as the reduction in moment arm and stability index could then be determined. To perform these simulations, I will define a 3D curve to simulate the tear geometry, remesh

the exposed supraspinatus tendon to align the elements along the tear, and reduce the number of attachment faces to reflect the change in tendon footprint. I can then run similar analyses to those presented in this dissertation. Another closely related question is to determine under what conditions a partial thickness tear is likely to progress, requiring surgical repair, or when it is unlikely to progress.

Simulate the effects of altered kinematics

We implemented the shoulder rhythm based on the most comprehensive kinematic data currently available for normal scapular and clavicular motion[22]. However, in a pathological case, bone motion can be far from normal. By changing the bone boundary conditions, we can redefine the shoulder rhythm based on kinematic data from impaired subjects. Running simulations with the finite element model would allow us to investigate how altered kinematics affect the ability of muscles to produce force.

Add cartilage and make the joint contact driven

Currently, we have restricted the model to be moved kinematically, and the resulting stresses and strains are calculated. These stresses are generated from muscle force production, which is dependent on fiber length and activation. To achieve desired joint motion requires a very good estimate of the timing and magnitude of the muscle activations. Since we were interested in simulating precise motion patterns for the calculation of moment arms, we decided to specify the kinematics. We assumed that the glenohumeral joint is an ideal ball joint, but normal motion of the humeral head has been shown to translate 2 to 4 mm with respect to the glenoid[79]. Allowing the model to be

driven by muscle forces and activations, rather than input kinematics, would introduce a new set of research questions. These would include evaluating muscle timing and activation level, determining muscle contributions to joint moments, and the concavity compression mechanism of joint stabilization. A contact driven joint is very difficult to achieve with a line segment model because a sparse number of actuators apply large forces along a few lines of action. These force estimates must be extremely accurate or the model will not be stable. However, the finite element model has the additional stabilization through wrapping, and will likely be more forgiving of small errors in approximation of muscle activation. The articulating cartilage surfaces are currently treated as rigid in the finite element model, but could easily be changed to represent articular cartilage. This would provide an additional opportunity to test model accuracy by comparing joint reaction forces (magnitude and direction) to those measured *in vivo*[8].

Create models of additional shoulder muscles

There are many shoulder muscles which have not been included in this analysis. This is due to the computational cost of adding additional degrees of freedom to the solution, and does not imply that these muscles are not important to shoulder function. Trapezius, rhomboids, and serratus anterior are important scapular stabilizers. The long head of biceps brachii is considered a key source of glenohumeral joint stability[102]. Pectoralis major has enormous potential to rotate the shoulder, and is also considered a major destabilizer of the glenohumeral joint[60,74]. Latissmus dorsi, and triceps brachii are also important in shoulder function. These muscles are difficult to represent using traditional line segment models because they are either broad and flat with large

attachments, have branching heads with multiple insertions, or both. Adding some or all of these muscles to the existing finite element model would broaden our understanding of how muscle coordination must be used to generate stable motion.

Create additional shoulder models of different populations

Holzbaur et al.[46] showed that muscle strength scaled with muscle volume. For their cohort of subjects, female subjects had approximately half the muscle volume of their male counterparts. This difference in force producing capability is likely to influence joint mechanics, and the creation of a finite element model of a female shoulder would provide a way to test how generalizable our model is. The development of finite element models is currently far too time consuming for the creation of subject-specific models. If the male-female model comparison reveals large differences in model results, we could develop a suite of representative models from other populations (e.g. middle aged vs. young, different body types, etc.). This would give the pseudo-subject-specific ability to choose a model best suiting a particular subject's body type and/or stage in life. It is also possible that we may find that the model we have is general enough to apply broadly, and that multiple models are unnecessary.

Couple the finite element model with a traditional biomechanical shoulder model

One great advantage to line segment based biomechanical models is that they are much simpler, and thus are much less costly for running simulations. Because human joints are an over determined system having many more actuators than degrees of freedom, it is customary to solve for muscle activations and forces using an optimization

approach. This approach is too computationally costly to implement using a finite element model because it requires a large number of function evaluations, and finite element evaluations are not trivial to compute. However, Halloran et al.[38,39] have generated some hybrid models which combine the detail of finite elements to model the complexities of foot-floor interaction, and the speed of line segment models to calculate optimal muscle forces in walking simulations. They developed an efficient computational scheme which only used the finite element model for about 5% of the simulation steps. This type of approach would make it feasible to investigate more dynamic motions such as baseball pitching because we would have a better estimation of muscle activations. We used small activations in our simulations, but this is certainly not a reasonable assumption when looking at sporting applications.

Create a different parameterization of line segment based muscle models

The Hill type muscle model that most researchers use assumes uniform behavior for all fibers in a muscle region. The finite element models indicate that this is not an accurate assumption. A generalization could be made of this popular model in which input parameters (e.g. pennation angle) could vary within a range rather than being a single discrete value. This shoulder model of five muscles is probably not sufficient for generalizing the behavior of all skeletal muscle, but it provides a good starting point by characterizing the fiber level behavior of muscles that surround one important joint of the body.

3.2.2 Experimental projects

Representing muscle as a continuum of interconnected fibers requires a lot of input data. Not all of this data is readily available, and many parameters must be approximated. The proposed experimental work will either improve the accuracy of the input data or will be used for additional verification of the model results.

Collect architecture data for the broad muscles of the shoulder

Thorough architectural data has been published for the rotator cuff muscles[100]. Architectural data such as optimal fiber lengths, fiber operating ranges, fiber lengths, and moment arms are very sparse or nonexistent for some of the large, broad shoulder muscles. Some of the major muscles for which it would be beneficial to collect this data include pectoralis major, trapezius, latissimus dorsi, and serratus anterior. Optimal fiber length, which is based on sarcomere length, has been previously measured using laser diffraction[66,67]. Recent imaging advances have made it possible to use two-photon microscopy to image sarcomere lengths *in vivo*[70]. This is far less invasive than the surgical dissection required for laser diffraction. Both line segment and finite element models would benefit from knowing how optimal fiber lengths vary across broad muscles.

In addition, the finite element model requires that we define fiber trajectories within each muscle. Fiber paths of supraspinatus have been digitized[58], but this data does not exist for the rest of the shoulder muscles. In order to acquire physiologic 3D fiber trajectories, we could dissect and digitize the paths of the muscle fibers as Kim et al.[58] did. Diffusion tensor imaging (DTI) is another approach which may be more broadly

useful than digitizing fibers. DTI is a form of MR imaging which exploits the anisotropic structure of muscle by measuring water diffusion. This imaging, used with tractography, could be used to generate the 3D arrangement of muscle fibers[31]. This could lead to the creation of subject specific fiber trajectories that could be developed automatically for living subjects. This would improve both the accuracy, and the ease of model creation.

Image based verification of fiber strains

There are two medical imaging techniques which could be employed to test the accuracy of muscle strains predicted by the finite element model. Ultrasound is relatively inexpensive and widely available. It offers the ability to see the real-time deformation of muscle fascicles *in vivo*. It is reasonably portable, and could be used in conjunction with motion capture techniques to calculate local fascicle strain as a function of joint configuration. The disadvantage to ultrasound is that it only offers a 2D measure of strain, and it is difficult to maintain a consistent imaging plane. Another recently developed MRI technique is called 3D-Dense imaging[42,87,115] which can be used to calculate the 3D deformations of the tissues during a repetitive motion task. Due to the size constraints of an MRI bore, this would be a very limited range of motion for the shoulder, but would allow a 3D to 3D strain comparison.

Mechanical testing of along-fiber muscle compression characteristics

The common axiom is that muscles pull, but do not push. That is true from a sarcomere point of view, but when a whole muscle is axially compressed, there is definitely passive resistance present. A matrix term which represents this mode of

deformation needs to be added to the transversely isotropic material model used for muscle. Experimental axial compression testing needs to be done to discover the properties of muscle in this deformation mode.

3.2.3 Improvements to current modeling methods

The future work discussed in the following section will improve the accuracy, and extend the scope and applications of this shoulder model. This section focuses on further computational development.

Semi-automate the creation of subject specific meshes

The most time consuming part of this project has been the discretization of the muscles and tendons for the finite element mesh. The geometry of the muscles and tendons is complicated, and the pipeline for going from MRI images to finite element solutions takes weeks or months. This severely limits the feasibility of using a subject specific approach. It is not known which features of shoulder models are generalizable, so it would be ideal to create many models with different geometries. IAMesh is a freely available software tool developed at the University of Iowa, and has been used to morph existing template meshes to create subject specific finite element meshes of finger bones. Further exploration is needed to determine if high quality meshes of muscles and tendons can be generated through mesh morphing. If including internal tendon, the geometry is quite complex, and may not yield acceptable meshes. It may be even more beneficial to re-implement the constitutive model of muscle in a finite element solver which supports

tetrahedral elements. Tetrahedral elements can be generated automatically for complicated shapes which are difficult to represent with hexahedral elements.

Develop parallel algorithms to reduce computation time

Simulation time for the five muscles presented in this dissertation took between 6 and 30 hours. This makes it intractable to consider modeling all 20 muscles of the shoulder or to add additional chest, back, elbow, and forearm muscles. The recent paradigm in computer hardware is to increase speed by adding multiple cores and making computing parallel based. This trend has been accelerated by the introduction of programmable graphics processing units (GPU) which offer hundreds of processing cores and many thousands of threads available to developers. This has been demonstrated to offer speed increases of 8 to 50 times the processing speed of the CPU for various scientific codes. Nike3D[85] is an older finite element solver developed in Fortran. It would be extremely difficult to adapt Nike3D to exploit this shift in computer architecture. Therefore, I plan to convert my model to FEBio, an open source finite element solver written in a modern, object-oriented language. The muscle material model has already been implemented in FEBio, and has been tested to yield the same results as the muscle material in Nike3D. Additionally I plan to add GPU based parallel algorithms to the FEBio platform in order to decrease simulation times. Hopefully, with these optimizations, this model will continue to be a useful tool as computer hardware continues to develop and improve.

Develop graphically based fiber mapping software

The process of generating 3D muscle models currently requires many steps and many input files. The input to the fiber mapping routines in SIMM is a text file, and it can require a great deal of trial and error to generate a reasonable representation of the fiber trajectories. It is sometimes difficult to tell if the fiber layout could be improved, or to visualize how changing control points on a square template mesh will change the fiber patterns in 3D space. I plan to develop a graphically based 3D muscle model creation tool which will allow for loading and visualization of template and computational meshes. It will provide interactive, graphically based creation of fiber maps. This software will also be used to visualize simulation results and perform pre and post processing functions (such as writing output fiber vectors for each element, or moment arm calculations).

Establish a method for determining initial muscle stress and strain

We assume that there is no stress or strain when the system is in the neutral position. With this assumption we are not calculating absolute tissue strain, but changes in strain. If we are interested in the true stresses that a muscle experiences, we must account for this preloaded state. This is likely to be critical for the rotator cuff muscles where muscle fibers are generally stretched to their greatest length when the shoulder is in the neutral position. This is also the position where the cuff generates the most passive force, and so the initial stress is likely to be substantial for these muscles. We intend to implement the method described by Weiss et al.[104] which they used for finding initial stress in ligaments.

Use a multi-scale approach for muscle-tendon interactions

The current approach of modeling the muscle-tendon interface is to use two distinct material models and to direct the fibers orientations within the tendon and muscle to point in the same direction. This is a good first approximation, but having two neighboring dissimilar materials in a finite element model creates a stress concentration at the muscle-tendon interface. We know from microscopy that the fibers of the muscle and tendon interdigitate and form a connective layer. This would mean that the muscle to tendon interface is characterized by an intermediate material that softens this stress transition, rather than an abrupt change of material properties. This could be represented by a thin layer of hybrid material which transitions from muscle to tendon. This would involve modeling the interface on a much smaller scale than the whole muscle.

Extend the material model to include fatigue, remodeling, and wear

We have assumed that the shoulder is a static mechanical system which functions based on configuration alone. However, muscles are in a constant state of change, and there are many interesting questions in the areas of muscle fatigue, muscle adaptation and remodeling, effects of local micro-damage, and tendon wear. A common cause of shoulder pain is impingement of the supraspinatus tendon between the humeral head and the acromion. This contact is thought to wear tendons, and lead to cuff tears. Investigating the development of impingement wear would be an interesting and clinically relevant extension of the current modeling paradigm.

3.3 Summary

The research described in this dissertation provides a foundation for numerous projects which will further our understanding of muscle mechanics, and shoulder mechanics. We have developed the first 3D finite element model which is useful for characterizing muscle function in generating joint motion and joint stabilization. We applied the model to provide the most detailed moment arm calculations to date. It is my hope that this research will lead to improved treatment and diagnosis for shoulder injuries, and that further shoulder research will build on the groundwork which we have laid.

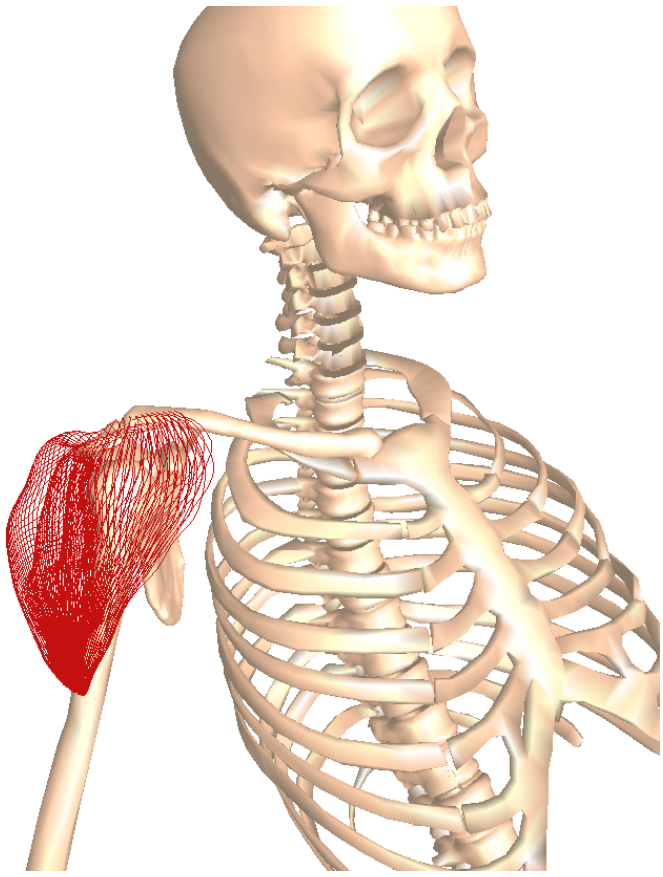

Figure 3.2 – Fiber representation of deltoid with the arm at 45° of abduction

References

1. Abboud, J. A. and Soslowsky, L. J. Interplay of the static and dynamic restraints in glenohumeral instability. *Clin Orthop Relat Res*(400):48-57, 2002.

2. Ackland, D. C., Pak, P., Richardson, M. and Pandy, M. G. Moment arms of the muscles crossing the anatomical shoulder. *J Anat* **213**(4):383-390, 2008.

3. Ackland, D. C. and Pandy, M. G. Lines of action and stabilizing potential of the shoulder musculature. *J Anat* **215**(2):184-197, 2009.

4. An, K. N., Takahashi, K., Harrigan, T. P. and Chao, E. Y. Determination of muscle orientations and moment arms. *J Biomech Eng* **106**(3):280-282, 1984.

5. Apreleva, M., Hasselman, C. T., Debski, R. E., Fu, F. H., Woo, S. L. and Warner, J. J. A dynamic analysis of glenohumeral motion after simulated capsulolabral injury. A cadaver model. *J Bone Joint Surg Am* **80**(4):474-480, 1998.

6. Apreleva, M., Parsons, I. M. t., Warner, J. J., Fu, F. H. and Woo, S. L. Experimental investigation of reaction forces at the glenohumeral joint during active abduction. *J Shoulder Elbow Surg* **9**(5):409-417, 2000.

7. Armfield, D. R., Stickle, R. L., Robertson, D. D., Towers, J. D. and Debski, R. E. Biomechanical basis of common shoulder problems. *Semin Musculoskelet Radiol* **7**(1):5-18, 2003.

8. Bergmann, G., Graichen, F., Bender, A., Kaab, M., Rohlmann, A. and Westerhoff, P. In vivo glenohumeral contact forces--measurements in the first patient 7 months postoperatively. *J Biomech* **40**(10):2139-2149, 2007.

9. Bitter, N. L., Clisby, E. F., Jones, M. A., Magarey, M. E., Jaberzadeh, S. and Sandow, M. J. Relative contributions of infraspinatus and deltoid during external rotation in healthy shoulders. *J Shoulder Elbow Surg* **16**(5):563-568, 2007.

10. Blana, D., Hincapie, J. G., Chadwick, E. K. and Kirsch, R. F. A musculoskeletal model of the upper extremity for use in the development of neuroprosthetic systems. *J Biomech* **41**(8):1714-1721, 2008.

11. Blana, D., Kirsch, R. F. and Chadwick, E. K. Combined feedforward and feedback control of a redundant, nonlinear, dynamic musculoskeletal system. *Med Biol Eng Comput* **47**(5):533-542, 2009.

12. Blemker, S. S., Asakawa, D. S., Gold, G. E. and Delp, S. L. Image-based musculoskeletal modeling: applications, advances, and future opportunities. *J Magn Reson Imaging* **25**(2):441-451, 2007.

13. Blemker, S. S. and Delp, S. L. Three-dimensional representation of complex muscle architectures and geometries. *Ann Biomed Eng* **33**(5):661-673, 2005.

14. Blemker, S. S. and Delp, S. L. Rectus femoris and vastus intermedius fiber excursions predicted by three-dimensional muscle models. *J Biomech* **39**(8):1383-1391, 2006.

15. Blemker, S. S., Pinsky, P. M. and Delp, S. L. A 3D model of muscle reveals the causes of nonuniform strains in the biceps brachii. *J Biomech* **38**(4):657-665, 2005.

16. Burkhart, S. S. The principle of margin convergence in rotator cuff repair as a means of strain reduction at the tear margin. *Ann Biomed Eng* **32**(1):166-170, 2004.

17. Burkhart, S. S. and Lo, I. K. Arthroscopic rotator cuff repair. *J Am Acad Orthop Surg* **14**(6):333-346, 2006.

18. Chadwick, E. K., Blana, D., van den Bogert, A. J. and Kirsch, R. F. A real-time, 3-D musculoskeletal model for dynamic simulation of arm movements. *IEEE Trans Biomed Eng* **56**(4):941-948, 2009.

19. Charlton, I. W. and Johnson, G. R. A model for the prediction of the forces at the glenohumeral joint. *Proc Inst Mech Eng H* **220**(8):801-812, 2006.

20. Criscione, J. C., Douglas, A. S. and Hunter, W. C. Physically based strain invariant set for materials exhibiting transversely isotropic behavior. *J Mech Phys Solids* **49**(4):871-897, 2001.

21. Dark, A., Ginn, K. A. and Halaki, M. Shoulder muscle recruitment patterns during commonly used rotator cuff exercises: an electromyographic study. *Phys Ther* **87**(8):1039-1046, 2007.

22. de Groot, J. H. and Brand, R. A three-dimensional regression model of the shoulder rhythm. *Clin Biomech (Bristol, Avon)* **16**(9):735-743, 2001.

23. De Sapio, V., Warren, J., Khatib, O. and Delp, S. Simulating the task-level control of human motion: a methodology and framework for implementation. *Visual Comput* **21**(5):289-302, 2005.

24. Delp, S. L., Anderson, F. C., Arnold, A. S., Loan, P., Habib, A., John, C. T., Guendelman, E. and Thelen, D. G. OpenSim: open-source software to create and analyze dynamic simulations of movement. *IEEE Trans Biomed Eng* **54**(11):1940-1950, 2007.

25. Delp, S. L., Loan, J. P., Hoy, M. G., Zajac, F. E., Topp, E. L. and Rosen, J. M. An interactive graphics-based model of the lower extremity to study orthopaedic surgical procedures. *IEEE Trans Biomed Eng* **37**(8):757-767, 1990.

26. Di Silvestro, M. D., Lo, I. K., Mohtadi, N., Pletsch, K. and Boorman, R. S. Patients undergoing stabilization surgery for recurrent, traumatic anterior shoulder instability commonly have restricted passive external rotation. *J Shoulder Elbow Surg* **16**(3):255-259, 2007.

27. Dickerson, C. R., Chaffin, D. B. and Hughes, R. E. A mathematical musculoskeletal shoulder model for proactive ergonomic analysis. *Comput Methods Biomech Biomed Engin* **10**(6):389-400, 2007.

28. Epstein, M., Wong, M. and Herzog, W. Should tendon and aponeurosis be considered in series? *J Biomech* **39**(11):2020-2025, 2006.

29. Fernandez, J. W., Buist, M. L., Nickerson, D. P. and Hunter, P. J. Modelling the passive and nerve activated response of the rectus femoris muscle to a flexion loading: a finite element framework. *Med Eng Phys* **27**(10):862-870, 2005.

30. Fernandez, J. W., Mithraratne, P., Thrupp, S. F., Tawhai, M. H. and Hunter, P. J. Anatomically based geometric modelling of the musculo-skeletal system and other organs. *Biomech Model Mechanobiol* **2**(3):139-155, 2004.

31. Galban, C. J., Maderwald, S., Uffmann, K., de Greiff, A. and Ladd, M. E. Diffusive sensitivity to muscle architecture: a magnetic resonance diffusion tensor imaging study of the human calf. *Eur J Appl Physiol* **93**(3):253-262, 2004.

32. Garner, B. A. and Pandy, M. G. Musculoskeletal model of the upper limb based on the visible human male dataset. *Comput Methods Biomech Biomed Engin* **4**(2):93-126, 2001.

33. Gatti, C. J., Dickerson, C. R., Chadwick, E. K., Mell, A. G. and Hughes, R. E. Comparison of model-predicted and measured moment arms for the rotator cuff muscles. *Clin Biomech (Bristol, Avon)* **22**(6):639-644, 2007.

34. Gold, G. E., Pappas, G. P., Blemker, S. S., Whalen, S. T., Campbell, G., McAdams, T. A. and Beaulieu, C. F. Abduction and external rotation in shoulder impingement: an open MR study on healthy volunteers initial experience. *Radiology* **244**(3):815-822, 2007.

35. Grana, W. A., Buckley, P. D. and Yates, C. K. Arthroscopic Bankart suture repair. *Am J Sports Med* **21**(3):348-353, 1993.

36. Halder, A. M., Halder, C. G., Zhao, K. D., O'Driscoll, S. W., Morrey, B. F. and An, K. N. Dynamic inferior stabilizers of the shoulder joint. *Clin Biomech (Bristol, Avon)* **16**(2):138-143, 2001.

37. Halder, A. M., Zhao, K. D., Odriscoll, S. W., Morrey, B. F. and An, K. N. Dynamic contributions to superior shoulder stability. *J Orthop Res* **19**(2):206-212, 2001.

38. Halloran, J. P., Ackermann, M., Erdemir, A. and van den Bogert, A. J. Concurrent musculoskeletal dynamics and finite element analysis predicts altered gait patterns to reduce foot tissue loading. *J Biomech* **43**(14):2810-2815, 2010.

39. Halloran, J. P., Erdemir, A. and van den Bogert, A. J. Adaptive surrogate modeling for efficient coupling of musculoskeletal control and tissue deformation models. *J Biomech Eng* **131**(1):011014, 2009.

40. Hayashida, K., Yoneda, M., Nakagawa, S., Okamura, K. and Fukushima, S. Arthroscopic Bankart suture repair for traumatic anterior shoulder instability: analysis of the causes of a recurrence. *Arthroscopy* **14**(3):295-301, 1998.

41. Herzog, W., Archambault, J. M., Leonard, T. R. and Nguyen, H. K. Evaluation of the implantable force transducer for chronic tendon-force recordings. *J Biomech* **29**(1):103-109, 1996.

42. Hess, A. T., Zhong, X., Spottiswoode, B. S., Epstein, F. H. and Meintjes, E. M. Myocardial 3D strain calculation by combining cine displacement encoding with stimulated echoes (DENSE) and cine strain encoding (SENC) imaging. *Magn Reson Med* **62**(1):77-84, 2009.

43. Hincapie, J. G., Blana, D., Chadwick, E. K. and Kirsch, R. F. Musculoskeletal model-guided, customizable selection of shoulder and elbow muscles for a C5 SCI neuroprosthesis. *IEEE Trans Neural Syst Rehabil Eng* **16**(3):255-263, 2008.

44. Hodges, P. W., Pengel, L. H., Herbert, R. D. and Gandevia, S. C. Measurement of muscle contraction with ultrasound imaging. *Muscle Nerve* **27**(6):682-692, 2003.

45. Holzbaur, K. R., Murray, W. M. and Delp, S. L. A model of the upper extremity for simulating musculoskeletal surgery and analyzing neuromuscular control. *Ann Biomed Eng* **33**(6):829-840, 2005.

46. Holzbaur, K. R., Murray, W. M., Gold, G. E. and Delp, S. L. Upper limb muscle volumes in adult subjects. *J Biomech* **40**(4):742-749, 2007.

47. Hughes, R. E., Niebur, G., Liu, J. and An, K. N. Comparison of two methods for computing abduction moment arms of the rotator cuff. *J Biomech* **31**(2):157-160, 1998.

48. Huijing, P. A. Muscle as a collagen fiber reinforced composite: a review of force transmission in muscle and whole limb. *J Biomech* **32**(4):329-345, 1999.

49. Huijing, P. A. Muscular force transmission necessitates a multilevel integrative approach to the analysis of function of skeletal muscle. *Exerc Sport Sci Rev* **31**(4):167-175, 2003.

50. Huijing, P. A. and Baan, G. C. Extramuscular myofascial force transmission within the rat anterior tibial compartment: proximo-distal differences in muscle force. *Acta Physiol Scand* **173**(3):297-311, 2001.

51. Inman, V. T., Saunders, J. B. D. and Abbott, L. C. Observations on the function of the shoulder joint. *J Bone Joint Surg* **26**:1-30, 1944.

52. Itoi, E., Newman, S. R., Kuechle, D. K., Morrey, B. F. and An, K. N. Dynamic anterior stabilisers of the shoulder with the arm in abduction. *J Bone Joint Surg Br* **76**(5):834-836, 1994.

53. Johansson, T., Meier, P. and Blickhan, R. A finite-element model for the mechanical analysis of skeletal muscles. *J Theor Biol* **206**(1):131-149, 2000.

54. Jones, M. Bilateral anterior dislocation of the shoulders due to the bench press. *Br J Sports Med* **21**(3):139, 1987.

55. Juul-Kristensen, B., Bojsen-Moller, F., Finsen, L., Eriksson, J., Johansson, G., Stahlberg, F. and Ekdahl, C. Muscle sizes and moment arms of rotator cuff muscles determined by magnetic resonance imaging. *Cells Tissues Organs* **167**(2-3):214-222, 2000.

56. Juul-Kristensen, B., Bojsen-Moller, F., Holst, E. and Ekdahl, C. Comparison of muscle sizes and moment arms of two rotator cuff muscles measured by ultrasonography and magnetic resonance imaging. *Eur J Ultrasound* **11**(3):161-173, 2000.

57. Kido, T., Itoi, E., Lee, S. B., Neale, P. G. and An, K. N. Dynamic stabilizing function of the deltoid muscle in shoulders with anterior instability. *Am J Sports Med* **31**(3):399-403, 2003.

58. Kim, S. Y., Boynton, E. L., Ravichandiran, K., Fung, L. Y., Bleakney, R. and Agur, A. M. Three-dimensional study of the musculotendinous architecture of supraspinatus and its functional correlations. *Clin Anat* **20**(6):648-655, 2007.

59. Klein Breteler, M. D., Spoor, C. W. and Van der Helm, F. C. Measuring muscle and joint geometry parameters of a shoulder for modeling purposes. *J Biomech* **32**(11):1191-1197, 1999.

60. Labriola, J. E., Lee, T. Q., Debski, R. E. and McMahon, P. J. Stability and instability of the glenohumeral joint: the role of shoulder muscles. *J Shoulder Elbow Surg* **14**(1 Suppl S):32S-38S, 2005.

61. Langenderfer, J. E., Patthanacharoenphon, C., Carpenter, J. E. and Hughes, R. E. Variation in external rotation moment arms among subregions of supraspinatus, infraspinatus, and teres minor muscles. *J Orthop Res* **24**(8):1737-1744, 2006.

62. Lee, S. B. and An, K. N. Dynamic glenohumeral stability provided by three heads of the deltoid muscle. *Clin Orthop Relat Res*(400):40-47, 2002.

63. Lee, S. B., Itoi, E., O'Driscoll, S. W. and An, K. N. Contact geometry at the undersurface of the acromion with and without a rotator cuff tear. *Arthroscopy* **17**(4):365-372, 2001.

64. Lee, S. B., Kim, K. J., O'Driscoll, S. W., Morrey, B. F. and An, K. N. Dynamic glenohumeral stability provided by the rotator cuff muscles in the mid-range and end-range of motion. A study in cadavera. *J Bone Joint Surg Am* **82**(6):849-857, 2000.

65. Lemos, R. R., Epstein, M. and Herzog, W. Modeling of skeletal muscle: the influence of tendon and aponeuroses compliance on the force-length relationship. *Med Biol Eng Comput* **46**(1):23-32, 2008.

66. Lieber, R. L., Loren, G. J. and Friden, J. In vivo measurement of human wrist extensor muscle sarcomere length changes. *J Neurophysiol* **71**(3):874-881, 1994.

67. Lieber, R. L., Yeh, Y. and Baskin, R. J. Sarcomere length determination using laser diffraction. Effect of beam and fiber diameter. *Biophys J* **45**(5):1007-1016, 1984.

68. Liu, J., Hughes, R. E., Smutz, W. P., Niebur, G. and Nan-An, K. Roles of deltoid and rotator cuff muscles in shoulder elevation. *Clin Biomech (Bristol, Avon)* **12**(1):32-38, 1997.

69. Liu, M. Q., Anderson, F. C., Schwartz, M. H. and Delp, S. L. Muscle contributions to support and progression over a range of walking speeds. *J Biomech* **41**(15):3243-3252, 2008.

70. Llewellyn, M. E., Barretto, R. P., Delp, S. L. and Schnitzer, M. J. Minimally invasive high-speed imaging of sarcomere contractile dynamics in mice and humans. *Nature* **454**(7205):784-788, 2008.

71. Lu, Y. T., Zhu, H. X., Richmond, S. and Middleton, J. Modelling skeletal muscle fibre orientation arrangement. *Comput Methods Biomech Biomed Engin*:1, 2010.

72. Maas, H., Baan, G. C. and Huijing, P. A. Intermuscular interaction via myofascial force transmission: effects of tibialis anterior and extensor hallucis longus length on force transmission from rat extensor digitorum longus muscle. *J Biomech* **34**(7):927-940, 2001.

73. Maganaris, C. N. Imaging-based estimates of moment arm length in intact human muscle-tendons. *Eur J Appl Physiol* **91**(2-3):130-139, 2004.

74. McMahon, P. J. and Lee, T. Q. Muscles may contribute to shoulder dislocation and stability. *Clinical orthopaedics and related research*(403 Suppl):S18-25, 2002.

75. Meskers, C. G., van der Helm, F. C., Rozendaal, L. A. and Rozing, P. M. In vivo estimation of the glenohumeral joint rotation center from scapular bony landmarks by linear regression. *J Biomech* **31**(1):93-96, 1998.

76. Mishra, D. K. and Fanton, G. S. Two-year outcome of arthroscopic bankart repair and electrothermal-assisted capsulorrhaphy for recurrent traumatic anterior shoulder instability. *Arthroscopy* **17**(8):844-849, 2001.

77. Napadow, V. J., Chen, Q., Mai, V., So, P. T. and Gilbert, R. J. Quantitative analysis of three-dimensional-resolved fiber architecture in heterogeneous skeletal muscle tissue using nmr and optical imaging methods. *Biophys J* **80**(6):2968-2975, 2001.

78. Novotny, J. E., Nichols, C. E. and Beynnon, B. D. Kinematics of the glenohumeral joint with Bankart lesion and repair. *J Orthop Res* **16**(1):116-121, 1998.

79. Novotny, J. E., Nichols, C. E. and Beynnon, B. D. Normal kinematics of the unconstrained glenohumeral joint under coupled moment loads. *J Shoulder Elbow Surg* **7**(6):629-639, 1998.

80. Oberhofer, K., Mithraratne, K., Stott, N. S. and Anderson, I. A. Anatomically-based musculoskeletal modeling: prediction and validation of muscle deformation during walking. *Visual Comput* **25**(9):843-851, 2009.

81. Otis, J. C., Jiang, C. C., Wickiewicz, T. L., Peterson, M. G., Warren, R. F. and Santner, T. J. Changes in the moment arms of the rotator cuff and deltoid muscles with abduction and rotation. *J Bone Joint Surg Am* **76**(5):667-676, 1994.

82. Pappas, G. P., Asakawa, D. S., Delp, S. L., Zajac, F. E. and Drace, J. E. Nonuniform shortening in the biceps brachii during elbow flexion. *J Appl Physiol* **92**(6):2381-2389, 2002.

83. Park, D. Y., Rubenson, J., Carr, A., Mattson, J., Besier, T. and Chou, L. B. Influence of stretching and warm-up on Achilles tendon material properties. *Foot Ankle Int* **32**(4):407-413, 2011.

84. Prompers, J. J., Jeneson, J. A., Drost, M. R., Oomens, C. C., Strijkers, G. J. and Nicolay, K. Dynamic MRS and MRI of skeletal muscle function and biomechanics. *NMR Biomed* **19**(7):927-953, 2006.

85. Puso, M. A., Maker, B. N., Ferencz, R. M. and Hallquist, J. O. Nike3D: A Non-linear, Implicit, Three-Dimensional Finite Element Code for Solid and Structural Mechanics. *Lawrence Livermore National Laboratory Technical Report*, 2002.

86. Saul, K. R., Murray, W. M., Hentz, V. R. and Delp, S. L. Biomechanics of the Steindler flexorplasty surgery: a computer simulation study. *J Hand Surg Am* **28**(6):979-986, 2003.

87. Spottiswoode, B. S., Zhong, X., Lorenz, C. H., Mayosi, B. M., Meintjes, E. M. and Epstein, F. H. 3D myocardial tissue tracking with slice followed cine DENSE MRI. *J Magn Reson Imaging* **27**(5):1019-1027, 2008.

88. Tempelhof, S., Rupp, S. and Seil, R. Age-related prevalence of rotator cuff tears in asymptomatic shoulders. *J Shoulder Elbow Surg* **8**(4):296-299, 1999.

89. Teran, J., Sifakis, E., Blemker, S. S., Ng-Thow-Hing, V., Lau, C. and Fedkiw, R. Creating and simulating skeletal muscle from the visible human data set. *IEEE Trans Vis Comput Graph* **11**(3):317-328, 2005.

90. Thelen, D. G., Anderson, F. C. and Delp, S. L. Generating dynamic simulations of movement using computed muscle control. *J Biomech* **36**(3):321-328, 2003.

91. Tingart, M. J., Apreleva, M., Lehtinen, J. T., Capell, B., Palmer, W. E. and Warner, J. J. Magnetic resonance imaging in quantitative analysis of rotator cuff muscle volume. *Clin Orthop Relat Res*(415):104-110, 2003.

92. van der Helm, F. C. A finite element musculoskeletal model of the shoulder mechanism. *J Biomech* **27**(5):551-569, 1994.

93. van der Helm, F. C. and Veeger, H. E. Quasi-static analysis of muscle forces in the shoulder mechanism during wheelchair propulsion. *J Biomech* **29**(1):39-52, 1996.

94. van der Helm, F. C., Veeger, H. E., Pronk, G. M., Van der Woude, L. H. and Rozendal, R. H. Geometry parameters for musculoskeletal modelling of the shoulder system. *J Biomech* **25**(2):129-144, 1992.

95. van der Helm, F. C. and Veenbaas, R. Modelling the mechanical effect of muscles with large attachment sites: application to the shoulder mechanism. *J Biomech* **24**(12):1151-1163, 1991.

96. van der Woude, L. H., Veeger, H. E., Dallmeijer, A. J., Janssen, T. W. and Rozendaal, L. A. Biomechanics and physiology in active manual wheelchair propulsion. *Med Eng Phys* **23**(10):713-733, 2001.

97. Veeger, H. E., van der Woude, L. H. and Rozendal, R. H. Load on the upper extremity in manual wheelchair propulsion. *J Electromyogr Kinesiol* **1**(4):270-280, 1991.

98. Veeger, H. E., Yu, B., An, K. N. and Rozendal, R. H. Parameters for modeling the upper extremity. *J Biomech* **30**(6):647-652, 1997.

99. Vermeiren, J., Handelberg, F., Casteleyn, P. P. and Opdecam, P. The rate of recurrence of traumatic anterior dislocation of the shoulder. A study of 154 cases and a review of the literature. *Int Orthop* **17**(6):337-341, 1993.

100. Ward, S. R., Hentzen, E. R., Smallwood, L. H., Eastlack, R. K., Burns, K. A., Fithian, D. C., Friden, J. and Lieber, R. L. Rotator cuff muscle architecture: implications for glenohumeral stability. *Clin Orthop Relat Res* **448**:157-163, 2006.

101. Warner, J. J., Bowen, M. K., Deng, X., Torzilli, P. A. and Warren, R. F. Effect of joint compression on inferior stability of the glenohumeral joint. *J Shoulder Elbow Surg* **8**(1):31-36, 1999.

102. Warner, J. J. and McMahon, P. J. The role of the long head of the biceps brachii in superior stability of the glenohumeral joint. *J Bone Joint Surg Am* **77**(3):366-372, 1995.

103. Weber, S. C., Abrams, J. S. and Nottage, W. M. Complications associated with arthroscopic shoulder surgery. *Arthroscopy* **18**(2 Suppl 1):88-95, 2002.

104. Weiss, J. A., Gardiner, J. C., Ellis, B. J., Lujan, T. J. and Phatak, N. S. Three-dimensional finite element modeling of ligaments: technical aspects. *Med Eng Phys* **27**(10):845-861, 2005.

105. Weiss, J. A., Maker, B. N. and Govindjee, S. Finite element implementation of incompressible, transversely isotropic hyperelasticity. *Comput Method Appl M* **135**(1-2):107-128, 1996.

106. Westerhoff, P., Graichen, F., Bender, A., Halder, A., Beier, A., Rohlmann, A. and Bergmann, G. In vivo measurement of shoulder joint loads during activities of daily living. *J Biomech* **42**(12):1840-1849, 2009.

107. Westerhoff, P., Graichen, F., Bender, A., Rohlmann, A. and Bergmann, G. An instrumented implant for in vivo measurement of contact forces and contact moments in the shoulder joint. *Med Eng Phys* **31**(2):207-213, 2009.

108. Wu, G., van der Helm, F. C., Veeger, H. E., Makhsous, M., Van Roy, P., Anglin, C., Nagels, J., Karduna, A. R., McQuade, K., Wang, X., Werner, F. W. and Buchholz, B. ISB recommendation on definitions of joint coordinate systems of various joints for the reporting of human joint motion--Part II: shoulder, elbow, wrist and hand. *J Biomech* **38**(5):981-992, 2005.

109. Wuelker, N., Korell, M. and Thren, K. Dynamic glenohumeral joint stability. *J Shoulder Elbow Surg* **7**(1):43-52, 1998.

110. Yamamoto, N., Muraki, T., Sperling, J. W., Steinmann, S. P., Itoi, E., Cofield, R. H. and An, K. N. Contact between the coracoacromial arch and the rotator cuff tendons in nonpathologic situations: a cadaveric study. *J Shoulder Elbow Surg* **19**(5):681-687, 2010.

111. Yanagawa, T., Goodwin, C. J., Shelburne, K. B., Giphart, J. E., Torry, M. R. and Pandy, M. G. Contributions of the individual muscles of the shoulder to glenohumeral joint stability during abduction. *J Biomech Eng* **130**(2):021024, 2008.

112. Yucesoy, C. A., Koopman, B. H., Baan, G. C., Grootenboer, H. J. and Huijing, P. A. Effects of inter- and extramuscular myofascial force transmission on adjacent

synergistic muscles: assessment by experiments and finite-element modeling. *J Biomech* **36**(12):1797-1811, 2003.

113. Yucesoy, C. A., Koopman, B. H., Huijing, P. A. and Grootenboer, H. J. Three-dimensional finite element modeling of skeletal muscle using a two-domain approach: linked fiber-matrix mesh model. *J Biomech* **35**(9):1253-1262, 2002.

114. Zajac, F. E. Muscle and tendon: properties, models, scaling, and application to biomechanics and motor control. *Crit Rev Biomed Eng* **17**(4):359-411, 1989.

115. Zhong, X., Spottiswoode, B. S., Meyer, C. H., Kramer, C. M. and Epstein, F. H. Imaging three-dimensional myocardial mechanics using navigator-gated volumetric spiral cine DENSE MRI. *Magn Reson Med* **64**(4):1089-1097, 2010.

116. Zhou, H. and Novotny, J. E. Cine phase contrast MRI to measure continuum Lagrangian finite strain fields in contracting skeletal muscle. *J Magn Reson Imaging* **25**(1):175-184, 2007.